Glacial runoff modulates 21st century basin aridity, but models disagree on the details

Lizz Ultee[1,1,1] and Sloan Coats[2,2,2]

[1]Massachusetts Institute of Technology
[2]University of Hawaii

November 30, 2022

Abstract

Global climate model projections suggest that 21st century climate change will bring significant drying in the midlatitudes. Recent glacier modeling suggests that runoff from glaciers will continue to provide substantial freshwater in many drainage basins, though the supply will generally diminish throughout the century. In the absence of dynamic glacier ice within global climate models (GCMs), a comprehensive picture of future basin-scale water availability for human and ecosystem services has been elusive. Here, we leverage the results of existing GCMs and a global glacier model to compute the effect of glacial runoff on the Standardized Precipitation-Evapotranspiration Index (SPEI), an indicator of basin-scale water availability. We find that glacial runoff tends to increase mean SPEI and reduce interannual variability, even in basins with relatively little glacier cover. However, in many basins we find inter-GCM spread comparable to the amplitude of the ensemble mean glacial effect, which suggests considerable structural uncertainty.

Glacial runoff buffers drought through the 21st century—but models disagree on the details

Lizz Ultee[1], Sloan Coats[2]

[1]Massachusetts Institute of Technology, Dept. of Earth, Atmospheric, and Planetary Sciences
[2]University of Hawaii at Manoa, Dept. of Earth Sciences

Key Points:

- We compute the effect of glacial runoff on the Standardized Precipitation-Evapotranspiration Index for 56 glaciated basins worldwide.
- In general, accounting for glacial runoff increases mean SPEI and decreases variance.
- Projected 21st-century changes in basin hydroclimate both with and without glacial runoff show wide variation across models.

Corresponding author: Lizz Ultee, `ehultee@umich.edu`

Abstract

Global climate model projections suggest that 21st century climate change will bring significant drying in the midlatitudes. Recent glacier modeling suggests that runoff from glaciers will continue to provide substantial freshwater in many drainage basins, though the supply will generally diminish throughout the century. In the absence of dynamic glacier ice within global climate models (GCMs), a comprehensive picture of future basin-scale water availability for human and ecosystem services has been elusive. Here, we leverage the results of existing GCMs and a global glacier model to compute the effect of glacial runoff on the Standardized Precipitation-Evapotranspiration Index (SPEI), an indicator of basin-scale water availability. We find that glacial runoff tends to increase mean SPEI and reduce interannual variability, even in basins with relatively little glacier cover. However, in many basins we find inter-GCM spread comparable to the amplitude of the ensemble mean glacial effect, which suggests considerable structural uncertainty.

Plain Language Summary

Mountain glaciers accumulate water during cooler, wetter seasons and release water during warmer, drier seasons. The seasonal pattern of freshwater release from glaciers, offset from the typical seasonal pattern of precipitation, makes them an important source of freshwater for mountainous regions around the world. Computer simulations have shown that the supply of freshwater from glaciers is likely to change as the climate changes. Separately, global climate model simulations suggest that many regions will experience more drought in the coming decades due to changes in the global water cycle. To understand what consequences those changes could have for on-the-ground water availability, we analysed existing glacier simulations together with global climate model simulations. We calculated the Standardized Precipitation-Evapotranspiration Index (SPEI), which quantifies drought conditions. We found that including glacial meltwater and runoff in the calculation of SPEI could reduce drought throughout the 21st century in many regions. The glacial effect becomes weaker as glaciers shrink due to climate change. However, the strength of the effect over time varies from one global climate model to another. Motivated by these results, we identify priority areas for model development to improve understanding of the glacial buffering effect on drought.

1 Introduction

Global climate model projections suggest that on large scales the terrestrial midlatitudes will experience significant drying over the coming century (Cook et al., 2014, 2020), although there are uncertainties related to the choice of hydroclimate metric and the role of land surface processes in driving those changes (Milly & Dunne, 2016; Swann et al., 2016; Scheff et al., 2017; Mankin et al., 2018; Yang et al., 2019; Mankin et al., 2019; Ault, 2020). While ongoing model development has improved the treatment of key climate processes that shape water availability for human and ecosystem services ("hydroclimate processes"), a number of factors remain difficult to capture, particularly those at regional and smaller spatial scales. For instance, current global climate models do not account for changing glacier volume and extent, with important consequences for projections of future water availability in glaciated regions (Barnett et al., 2005). Runoff from mountain glaciers can account for a significant proportion of dry-season water supply in arid regions (Vergara et al., 2007; Soruco et al., 2015; Pritchard, 2019). Future glacier runoff depends on nonlinear glacier-dynamic response to changing climate (Huss & Hock, 2018; Marzeion et al., 2020), which cannot be simulated directly in global climate models nor extrapolated from observations. Moreover, the importance of glacial runoff for water supply differs with regional climate (Kaser et al., 2010; Immerzeel et al., 2010; Rowan et al., 2018), emphasising the need for a holistic view of glaciated-basin hydroclimate change.

The use of state-of-the-art global climate models (GCMs) to project hydroclimate change is appealing because the simulated changes reflect self-consistent climate physics on the global-to-regional scale. Nevertheless, the climate physics simulated by each GCM are an uncertain approximation of those in the real world. Intercomparisons of multiple GCMs allow for a quantification of the range of projections that result from the uncertain approximations made by each—so called structural uncertainty. These quantifications are hindered, however, by the incomparability of directly-simulated hydroclimate quantities across GCMs. For example, the land components of GCMs range widely in complexity, including different numbers of soil levels with inconsistent corresponding depths (e.g. Cook et al., 2014) and widely varying runoff sensitivities (e.g. Lehner et al., 2019). The resulting difficulty in comparing hydroclimate metrics directly across GCMs has led to the widespread use of offline hydroclimate metrics when quantifying hydroclimate change, specifically in the form of standardized drought indices that facilitate like-for-like intercomparison.

Among the drought indices in operational use (reviewed by World Meteorological Organization & Global Water Partnership, 2016), only a few are globally intercomparable, scalable for different types of drought, and applicable under a variety of future climate change scenarios. For example, the widely-used Palmer Drought Severity Index (PDSI; Palmer, 1965) has a single inherent timescale of approximately nine months, which limits its applicability to certain types of drought conditions. The Standardized Precipitation Index (SPI; McKee et al., 1993) is more flexible, but its lack of consideration for atmospheric moisture demand limits its applicability to future climate chnage. The Standardized Precipitation-Evapotranspiration Index (SPEI; Vicente-Serrano et al., 2009) satisfies all of the above criteria and offers a user-defined temporal scale to facilitate studies of hydroclimate variability across timescales and climate system components (e.g. Lorenzo-Lacruz et al., 2010; Potop et al., 2012; Kingston et al., 2014; Ault, 2020). SPEI is regularly computed at the coarse spatial resolutions typical of GCMs, both for operational drought monitoring and forecasting and for projections of drought conditions in a changing climate (Cook et al., 2014). In semi-arid mountain regions—where glacial runoff is most likely to be an important water source—SPEI realistically captures hydrological drought at timescales of 11 to 15 months (McEvoy et al., 2012; Jiang et al., 2017).

The analysis of GCM-derived drought indices depends on reliable simulation of hydroclimate. The representation of land surface processes, including those related to vegetation, remains a source of uncertainty in hydroclimate projections (Mankin et al., 2017, 2019; Lehner et al., 2019). In many cases, GCM land components are not equipped to handle the hydrology of glaciated drainage basins on the century scale. The MATSIRO land surface model (Takata et al., 2003) used in MIROC-ESM, for example, handles water routing through snowpack, but not multiannual storage in glacier ice. The land surface scheme of CNRM-CM6 allows limited water storage in snow and ice and includes a "permanent snow/ice" land tile classification (Decharme et al., 2019), but cannot resolve changes in ice cover over time. GCMs including CCSM and NorESM use the Community Land Model (CLM) to simulate land-surface dynamics and hydrology. CLM includes glacier ice among its land-cover types, but does not account for glacier dynamics or change over time (Lawrence et al., 2018). Further, the spatial resolution of current GCMs leaves them poorly equipped to handle precipitation gradients in high-relief areas (Flato et al., 2013), where mid-latitude glaciers are most likely to be found. Global glacier models have demonstrated that glacier coverage worldwide cannot be assumed static over the coming century (Huss & Hock, 2018; Marzeion et al., 2018, 2020); thus, surface hydrology schemes that do not account for changing glacial water storage over time risk under- or over-estimating the true water availability (van de Wal & Wild, 2001).

There have been substantial recent efforts to quantify 21st-century changes in glacial water runoff at global (Bliss et al., 2014; Huss & Hock, 2018; Marzeion et al., 2018; Cáceres et al., 2020) and regional scales (Juen et al., 2007; Immerzeel et al., 2012; Schaefli et al., 2019; Brunner et al., 2019; Mackay et al., 2019). To understand how these changes will translate to changing basin-scale water availability for human and ecosystem services, however, requires the added context of regional hydroclimate variability and change (Kaser et al., 2010). Here, we quantify the glacial effect on future hydroclimate change, as indicated by SPEI, for all 56 large-scale glaciated drainage basins (hereinafter "basins") worldwide.

2 Methods

We calculate SPEI following the methods of Cook et al. (2014, and see Supplementary Information). The index is a simple climatic water balance, with water accumulation through precipitation and loss through potential evapotranspiration (PET, calculated here following Allen et al., 1998), normalized such that its mean over a historical reference period is 0 and its standard deviation is 1. SPEI < 0 corresponds to drier conditions and SPEI > 0 to wetter conditions. Our approach isolates the glacial effect on SPEI using hydroclimate output of eight GCMs combined with offline simulated glacial runoff (Huss & Hock, 2018) forced by boundary conditions from the same GCMs. Although SPEI can be computed at multiple timescales, we focus here on the 15-month timescale because of its relevance to hydrological drought, which in turn is most relevant to water availability for human and ecosystem services.

We leverage existing glacier runoff estimates generated by Huss and Hock (2018) for all large-scale (> 5000 km^2) drainage basins in which present glacier ice coverage is at least 30 km^2 total and at least 0.01% of basin area. There are 56 such basins outside of Greenland and Antarctica. They comprise 16 basins in Asia, 11 in Europe, 16 in North America, 12 in South America, and 1 in New Zealand. Maps of basin location and projected change in glacier runoff appear in Huss and Hock (2018).

We identify eight GCMs that *(i)* provide the variables necessary to calculate SPEI and *(ii)* have a corresponding glacier-runoff projection from Huss and Hock (2018). For each GCM, we select the same representative concentration pathway (RCP) 4.5 and 8.5 simulations (Taylor et al., 2011) that were used to force projections in Huss and Hock (2018). From those GCM simulations, we extract atmospheric surface temperature, surface pressure, total precipitation, surface specific humidity, and surface net radiation for each of the 56 basins we study. Specifically, we identify all latitude-longitude grid points from the native GCM grid that fall within the boundary of the basin as defined by the Global Runoff Data Centre (2007), extract the required variables at each point, and then take the mean across grid points to produce a single timeseries for each variable in each basin. We then calculate PET with the basin mean timeseries for each variable using the reference crop approximation of Allen et al. (1998), and we calculate a second version with the addition of a stomatal conductance term (see Text S1.2) following Yang et al. (2019). We calculate SPEI with the resulting basin mean PET timeseries and the basin mean precipitation timeseries (see below and Text S1). Because some GCM grids have low spatial resolution, there are GCMs and basins where no data is available (15% of the total). Nevertheless, at least one GCM for each basin has data.

To test the role of glacial runoff in water availability as indicated by SPEI, we calculate two versions of the index. The first, SPEI$_N$, is calculated for each GCM in the standard way as described in Vicente-Serrano et al. (2009) and detailed in Supplementary Text S1, with no accounting for glacier change. For the second, SPEI$_W$, we account for glacier change by modifying the moisture source term in the calculation. We replace the total precipitation input p with

$$\tilde{p} = \frac{A - A_g}{A} p + \frac{A_g}{A} r, \tag{1}$$

where $\tilde{p}$ is the modified moisture source term, p is the initial moisture source term from each GCM with no glacial component, A_g is the initially glaciated area of the basin, A

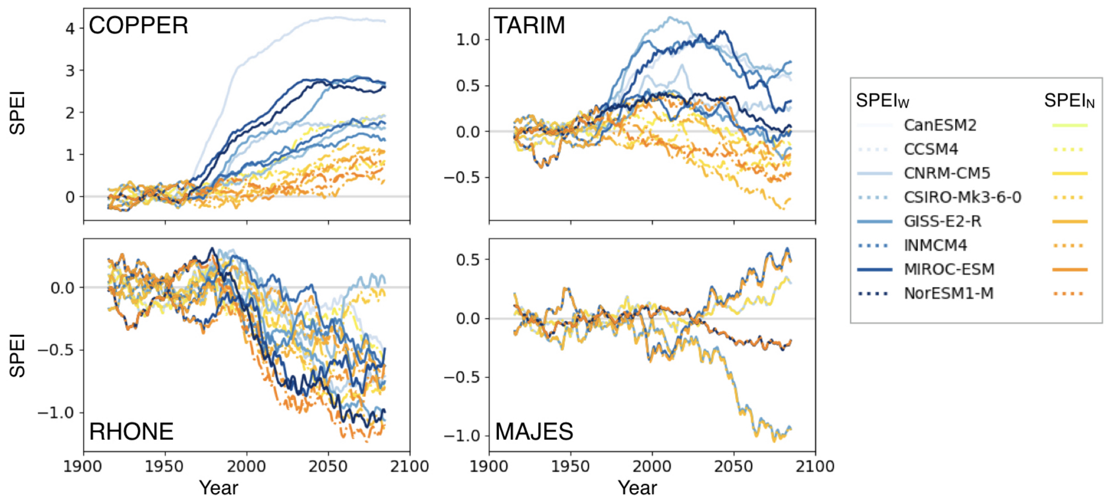

Figure 1. 30-year running mean time series of SPEI computed with each GCM with glacial runoff (blue shades) and without (orange shades) for the RCP 4.5 scenario in four example basins (name in corner of each figure panel).

is the total basin area, and r is the glacial runoff for that basin from Huss and Hock (2018) forced with the same GCM (see Supplementary Text S2). All terms apart from the moisture source terms $(p, \tilde{p})$ are consistent between SPEI_N and SPEI_W. Our modified SPEI calculation assumes that both precipitation and glacial runoff are distributed evenly across the drainage basin, which is a considerable simplification that we address further below.

The focus of our analysis is hydrological drought in glaciated basins. As such, we compute SPEI at the 15-month timescale on which it has been shown to capture hydrological drought in semi-arid, snowmelt-dependent mountain basins (e.g. McEvoy et al., 2012). At this timescale, SPEI should capture variability in streamflow, and specifically inflow to reservoirs, lakes, wetlands, and potentially groundwater (Vicente-Serrano et al., 2009); reductions of these inflows are called hydrological drought. Results for timescales between 3 and 27 months are available in our public repository for the reader interested in other types of drought or timescales of hydroclimate variability. Nevertheless, we caution that these other SPEI timescales may not reflect relevant hydroclimate processes in the basins we study.

For each GCM and basin, we compute and compare the 30-year running mean and variance of the SPEI_N and SPEI_W time series. We also take the difference of SPEI with and without glacial runoff (SPEI_W - SPEI_N) and compute running means of this difference for each basin. Finally, we compare GCM-by-GCM changes in SPEI mean and variance at the end of the 21st century (2070-2100) for RCP 4.5 and 8.5. We present results below for four geographically distributed basins: the Copper (North America), Tarim (Asia), Rhone (Europe), and Majes (South America). These basins are useful illustrations as they span the range of basin area glacial cover, span the range of glacial effect on SPEI, and have projected future SPEI with both drying and wetting trends. Results for all 56 basins appear in Supplementary Figures S2-S3 and our online repository. Results that are applicable to all GCMs, as well as inter-GCM uncertainties, are also described in the Results section and summarized in Figure 4.

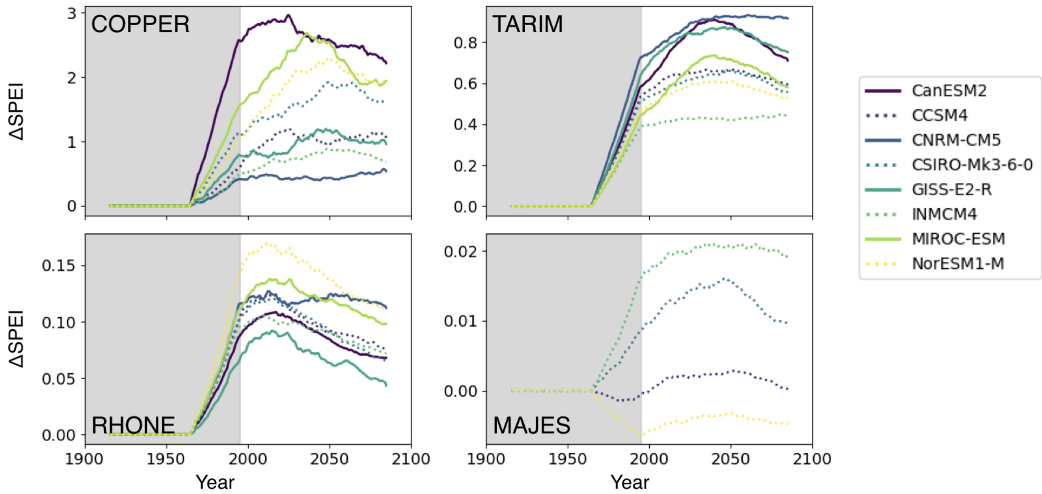

Figure 2. The effect on mean SPEI of including glacial runoff in four example basins, under emissions scenario RCP 4.5. Curves shown are a 30-year running mean of the difference SPEI_W-SPEI_N, where "W" and "N" denote "with glacial runoff" and "no accounting for glaciers", respectively. A different vertical scale has been applied to each plot to aid readability. Grey shading indicates the period when 30-year running means include years for which the glacier model has not yet been switched on.

3 Results

3.1 Glaciers reduce drought through the 21st century

Almost universally, accounting for glacial runoff results in an increase in mean SPEI. More specifically, there is unanimous GCM agreement that glacial runoff increases mean SPEI (i.e. makes conditions wetter in the mean) in 2070-2100 for 35 of the 56 basins tested. This is true for basins that are projected to dry throughout the century as well as those that are expected to become wetter. However, there is considerable variation in the temporal trends of the glacial effect on mean SPEI both across basins and between GCMs in a single basin.

Figure 1 shows the 30-year running-mean SPEI for four representative basins. The basins shown are geographically distributed, span the range of basin area glacial cover (A_g/A in Equation 1 above), and have projected future SPEI with both drying and wetting trends; results for all basins appear in the Supplementary Material. In the Copper River basin of Alaska, all eight GCMs project an increase in SPEI throughout the 21st century, with even more pronounced increases when glacial runoff is taken into account. In the Rhone basin of central Europe, most GCMs project decreasing SPEI throughout the century to be slightly mitigated by glacial runoff. The four GCMs available for the Majes basin of Peru (see Section 2) disagree about the temporal trend in SPEI, but none are much changed by the inclusion of glacial runoff. Most interesting is the Tarim basin of central Asia. When glacial runoff is not considered, all eight GCMs project SPEI to decrease throughout the 21st century, becoming negative on average after 2050. However, with glacial runoff included, GCMs show an initial increase in SPEI that remains positive (though decreasing) through the end of the century. This suggests that in the Tarim basin glacial runoff changes the projected future hydroclimate from one with less water availability for human and ecosystem services to one with greater water availability in the 21st relative to the 20th century.

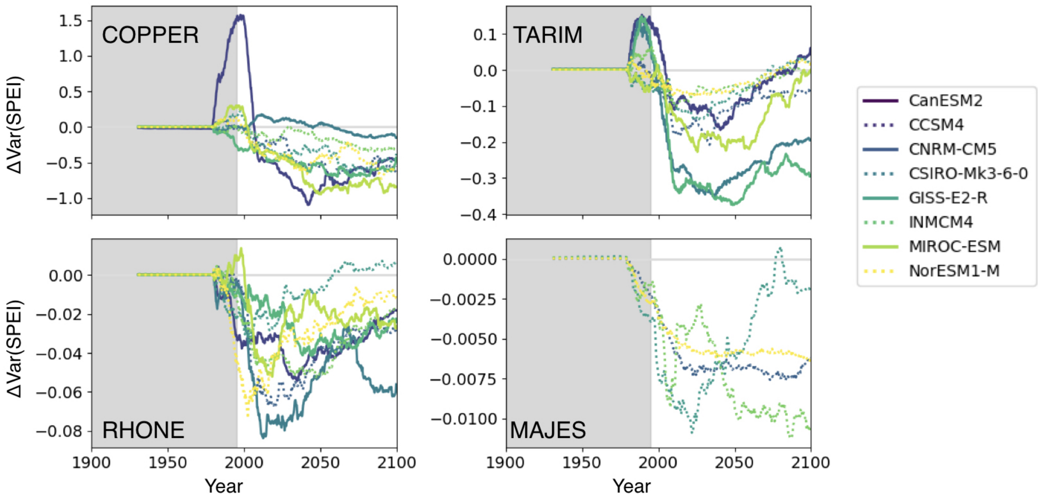

Figure 3. The effect on SPEI variance of including glacial runoff in four example basins, under emissions scenario RCP 4.5. Curves shown are the difference of running 30-year variances, Var(SPEI_W)-Var(SPEI_N), where "W" and "N" denote "with glacial runoff" and "no accounting for glaciers", respectively. A different vertical scale has been applied to each plot to aid readability. Grey shading indicates the period when 30-year running statistics include years for which the glacier model has not yet been switched on.

Isolating the glacial effect (Δ SPEI = SPEI_W - SPEI_N) in each basin further highlights the tendency for glacial runoff to increase mean SPEI, regardless of whether SPEI is projected to increase or decrease in the future (Figures 2 and S2). In the Copper basin, which is the most heavily glaciated of any we study ($A_g/A = 0.2001$) the glacial effect exceeds 1 SPEI unit and remains high throughout the 21st century. This means that the Copper basin is 1 standard deviation wetter on average with glacial runoff included, with the standard deviation being relative to interannual (15 month) variability over the late 20th century–in short, glacial runoff has a very large impact on average conditions in the Copper Basin. The glacial effect is also high, on the order of 1 SPEI unit, in the Tarim basin, even though the Tarim is an order of magnitude less glaciated ($A_g/A = 0.0234$) than the Copper. In the Rhone basin ($A_g/A = 0.0093$) there is a moderate glacial effect that declines throughout the century, and in the Majes basin ($A_g/A = 0.0031$) the glacial effect on SPEI is negligible. Figure S2 shows time series glacial effect for all basins analysed, and we report end-of-century multi-GCM ensemble glacial effect for all basins in Figure 4.

3.2 Glacial effect on SPEI variance is heterogeneous between basins

Figure 3 shows the effect on SPEI variance of including glacial runoff. In the Majes basin, the glacial effect on variance is just as negligible as the effect on mean SPEI. In the remaining three example basins, and in most other basins analysed (Supplementary Figure S3), adding glacial runoff to the SPEI calculation produces an initial increase in variance. This effect is more likely to be numerical than physical in nature, as it appears when 30-year running windows still include years with no glacier model input (shaded grey on Figure 3 and S3). After the initial increase, including glacial runoff decreases SPEI variance in the Copper, Rhone, and Tarim basins, in each case with a temporal trajectory that mirrors the increase in mean SPEI shown in Figure 2. In the Tarim and Rhone basins, where the glacial effect on mean SPEI begins to taper before the end of the century, some GCMs show a second increase in SPEI variance.

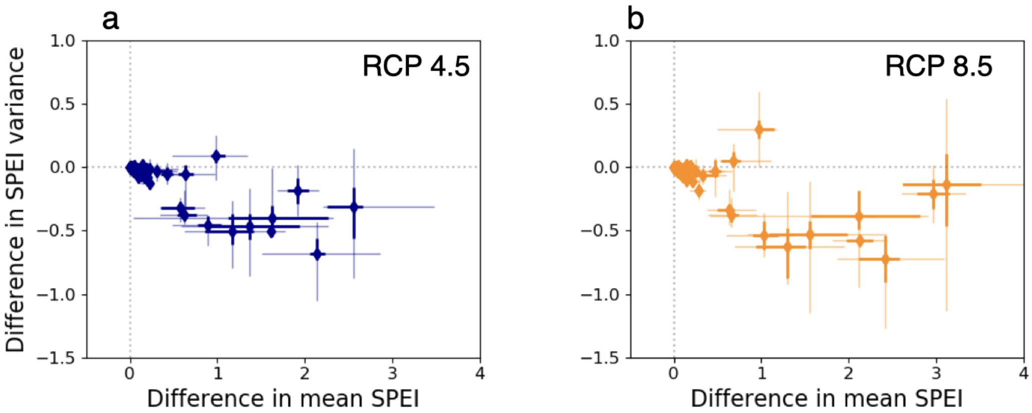

Figure 4. Difference due to explicit accounting of glacial runoff in SPEI 30-year mean and variance at end of 21st century (2070-2100), for climate scenarios RCP 4.5 (panel a) and RCP 8.5 (panel b). A diamond marker for each of the 56 basins analysed shows the difference in SPEI 30-year ensemble mean (x-axis) and variance (y-axis) for each basin. Whiskers show the range of single-GCM results for each basin, with interquartile range shaded.

Figure 4 confirms that accounting for glacial runoff decreases SPEI variance through the end of the 21st century in most basins. Under the more moderate RCP 4.5 climate scenario, there is only one basin for which all GCMs agree on the glacial effect being an increase in variance (positive y-axis values in Figure 4a; Figure S3). There are more projections of increased variance due to glacial runoff under the high-emissions RCP 8.5 climate scenario. The glacial effect on SPEI under RCP 8.5 also shows more heterogeneity among basins (wider dispersal of markers on Figure 4b) and among GCM projections (longer whiskers and wider interquartile range in Figure 4b). Nevertheless, on average, glacial runoff continues to provide a moderating influence through the end of the 21st century on both mean SPEI and the year-to-year SPEI variability that is typically associated with on-the-ground impacts.

4 Discussion

Huss and Hock (2018) found that the response of glacial runoff to 20th-21st century climate change took the shape of a bell curve, with maximum basin-level runoff ("peak water") occurring in some year after the onset of glacial retreat. Our analysis of SPEI$_N$ and SPEI$_W$ shows that in most basins, the effect of including glacial runoff is an increase in mean SPEI that diminishes later in the 21st century (Figure 2 and S2). This pattern is consistent with the "peak water" framing. We note, however, that the time evolution of the glacial effect on SPEI is not consistent across GCMs, with some GCMs showing a pronounced "peak" shape and others showing a "plateau" or a more steady slope (Figure 2 and S2). This inter-GCM spread is particularly evident in the Copper basin, where CanESM2 produces a large, sharp peak in glacial effect early in the century while MIROC-ESM produces a slower, nearly monotonic increase in the glacial effect on mean SPEI. Further, for several basins including the Copper and Tarim, even the end-of-century decline in glacial runoff does not return mean SPEI to values without glacial runoff. That is, the relevance of glaciers for future drought projections is not limited to this century.

Theoretical understanding suggests that interannual variance in water availability should be lower when basins have substantial glacial runoff, an effect known as glacial drought buffering (Fountain & Tangborn, 1985; Fleming & Clarke, 2005). While accounting for glacial runoff can produce an initial increase in SPEI variance (Figure 3 and S3), which is superficially inconsistent with the theoretical prediction, we find that the increase is a numerical artifact. In running windows that include some years before 1980 (when the glacier model is switched on) and some after, the sudden increase in mean SPEI with the introduction of glacial runoff manifests as an increase in variance. In subsequent years we find a reduction, on average, of SPEI variance due to glacial runoff (negative y-axis values in Figure 3, S3, and 4), which is consistent with the theoretical prediction. The glacial effect on variance weakens as glacial runoff decreases through the 21st century (smaller absolute values in Figure 3), supporting the prediction that glacial drought buffering will decline with 21st century climate change (Biemans et al., 2019). Under RCP 8.5, as compared to RCP 4.5, there are more GCMs and basins in which there is a weak end-of-century glacial effect on SPEI variance (negligible or even positive y-axis values in Figure 4b). We interpret that the greater warming under RCP 8.5 reduces seasonally-available meltwater (or "buffering capacity") due to the declining precipitation storage capacity of shrinking glaciers, such that the basin transitions to a precipitation-dependent regime. In short, the decline in buffering capacity happens faster with greater climate warming. However, in most basins and for most GCMs, glacial runoff remains effective in reducing SPEI variance at the end of the century under both RCP 4.5 and 8.5 (Figure 4).

In the context of current glacier-modelling efforts that show glacial runoff decreasing with continued climate change (Juen et al., 2007; Immerzeel et al., 2010; Marzeion et al., 2018; Huss & Hock, 2018), it has not previously been apparent that glaciers will continue to buffer droughts through the end of the 21st century. In qualitative assessments, both Rowan et al. (2018) and Pritchard (2019) found that current glacier meltwater production is unsustainably high in high-mountain Asia and that the glacial fraction of downstream runoff is likely to decline over the 21st century. Immerzeel et al. (2020) found that water stored in glaciers is an important resource of mountain "water towers" worldwide, and assessed that several glaciated basins are vulnerable to future change. However, each of these studies makes only indirect connections between future changes in glacier runoff and the additional hydroclimate processes that will shape future drought. Our SPEI analysis adds the basin-level hydroclimate context necessary to interpret future glacial drought buffering in a changed climate.

We assess that there are two categories of basins in which glacial effects are large and long-lived. The first category consists of heavily glaciated basins such as the Copper, where there is a large quantity of water stored as glacial ice. The second category consists of arid basins such as the Tarim, in which glacier runoff is a substantial water source. Basins in this category may not be heavily glaciated—the Tarim basin is only 2% glaciated by area—but other sources are sufficiently small that even limited glacial runoff has a pronounced effect on SPEI within the basin. Previous authors have also commented on the importance of glacial runoff in arid basins (Pritchard, 2019) and dry seasons (Soruco et al., 2015; Frans et al., 2016; Biemans et al., 2019).

The magnitude and temporal trajectory of the glacial effect varies not only by basin but also by GCM, as the examples in Figures 1 - 3 and S2-S3 illustrate. Of particular interest is that there is no consistent ordering to the GCM estimates of the glacial effect. That is, no one GCM of the eight we test is consistently wetter or drier, or more or less variable, when accounting for glacial runoff. Figures 2 and S2 also show that the glacial effect on SPEI peaks in different years for different GCMs. This inter-GCM heterogeneity reflects the complexity of basin-scale hydroclimate: The different treatments of the physical processes relevant to hydroclimate have implications for the glacial effect on SPEI despite each GCM driving the same glacier model of Huss and Hock (2018). For example, CanESM is the only GCM to use the Canadian Land Surface Scheme ("CLASS", Verseghy, 2000) and in the Copper basin CanESM has a glacial effect much stronger than any other model (Figure 2). Yet the same figure shows that glacial effects computed with

CCSM and NorESM, both of which account for (static) glacier ice cover in the same Community Land Model (Lawrence et al., 2018), but which utilize different atmospheric models, peak in different years and with different magnitudes. We deduce that there are processes within both land surface schemes and atmospheric model components of GCMs that must be addressed to account for dynamic glacier changes.

Two assumptions are inherent in our approach: first, that 15-month SPEI is an appropriate metric of variability in water supply for human and ecosystem services, and second, that glacial runoff and precipitation can be treated as evenly spatially distributed over the basin area for this purpose. The first assumption is justified by previous work on multi-scalar drought indices (Szalai et al., 2000; Vicente-Serrano & López-Moreno, 2005; Vicente-Serrano et al., 2009). In particular, the 15-month integration time scale we choose relates to variability in surface/ground water flows (see Methods and Supplementary Text S1.1) and has been shown to capture hydrological drought in semi-arid mountain basins (McEvoy et al., 2012). Our choice of temporal scale is also consistent with our second (spatial) assumption. Over time, heterogeneously-distributed glacial runoff and precipitation reaches humans and ecosystems—and becomes more evenly distributed over a basin—in several ways. For example, runoff localized in a stream could be diverted by irrigation infrastructure (Sorg et al., 2012), dammed for hydropower (Schaefli et al., 2019; Pritchard, 2019), or collected in a downstream reservoir serving a major city (e.g. La Paz, Bolivia; Soruco et al., 2015). Runoff could also recharge high-altitude wetlands (paramos) and groundwater aquifers (Liljedahl et al., 2017; Chidichimo et al., 2018; Somers et al., 2019; Vincent et al., 2019). Finally, runoff that remains as standing water on the surface, whether proglacial lakes or irrigation ponds, provides a ready source of moisture to the atmosphere, which can locally enhance precipitation and thereby spread water supply across the basin (de Kok et al., 2018). Directly modelling and accounting for these within-basin effects is beyond the scope of the present work, as well as current GCMs and glacier models. These considerations are part of the reason that hydrological drought is regularly quantified on the basin scale (e.g. Zhang et al., 2016; Leblanc et al., 2009, for the Yangtze and Murray-Darling basins, respectively) and SPEI is regularly computed at 100 km or lower spatial resolution (Cook et al., 2014). We assess that both assumptions inherent to our approach are justified in our interpretation of 15-month SPEI as an indicator of average water availability for human and ecosystem services in a basin.

We do not address uncertainty arising from the accounting of non-glacial processes within SPEI. For instance, the metric lacks explicit accounting of vegetation processes that could change the coupling of the land surface to the atmosphere under future climate change (Mankin et al., 2017, 2019; Lehner et al., 2019). It is unclear what role these vegetation processes play in the hydroclimate of the glaciated basins we analyse, particularly as relates to hydrological drought, and our results should be interpreted in the context of this uncertainty. Nevertheless, we have found that correcting the Penman-Montieth PET component of SPEI (Equation S.1) for greenhouse gas-driven changes in stomatal conductance and water use efficiency, as suggested by Yang et al. (2019), has a negligible impact on our results (Text S1.2).

The simple offline computation we present here helps account for the first-order glaciological effect on future basin-scale water availability for human and ecosystem services. However, offline computations are unable to capture atmospheric feedbacks of changing mountain glacier extent. For example, ice and snow-covered surfaces reflect more incident radiation to the atmosphere than bare rock or soil surfaces do. Water vapor sublimated from glacier ice or evaporated from supraglacial meltwater pools is a ready source of moisture to the local atmosphere. Finally, glacier surfaces are favorable for creation of strong downslope (katabatic) winds, which can be the dominant feature in local-scale atmospheric circulation (e.g. Obleitner, 1994; van den Broeke, 1997; Aizen et al., 2002). To the extent that any of these local processes are parameterized in current GCMs, their projection into the future will suffer from the inaccurate assumption that glacier ice cover is permanent. The effects of these feedbacks will only be resolved with eventual addition of fully coupled mountain glacier schemes in GCMs.

Here, we have focused on global intercomparison of future basin-scale water availability for human and ecosystem services. However, local-level water resource studies may benefit from more granular information (Milly et al., 2008; Head et al., 2011; Frans et al., 2016). Our method can be adapted for use with regional climate models (e.g. Noël et al., 2015; Skamarock et al., 2019), with models simulating individual glacier evolution (e.g. Gagliardini et al., 2013; Maussion et al., 2019; Rounce et al., 2020), and in probabilistic ensemble simulations (see Supplementary Text S3). The multiple temporal horizons of SPEI also make our method scalable, allowing analyses of different types of droughts and supporting eventual integrated physical-socioeconomic studies of the impacts of glacier change (Carey et al., 2017).

5 Conclusions

Basin-scale water availability as observed and experienced in the present is affected by numerous regionally-variable factors, including the supply of water from glaciers. GCMs in use to study past and future hydroclimate are ill-equipped to capture decade-to-century scale variation in glacial runoff. Although fully dynamic representations of glacier ice within GCMs will be necessary to produce a physically consistent projection of hydroclimate change in glaciated basins, we have presented a simple method to leverage recent glacier model developments (Huss & Hock, 2018) and account for changing glacial runoff in 21st-century projections of hydrological drought. Our analysis shows that applying glacier model output to account for glacial runoff in the SPEI tends to increase mean SPEI and reduce interannual variability in SPEI, even in basins with $< 2\%$ glaciation by area. As glaciers continue to retreat late in the century, their "drought buffering" effect on SPEI diminishes but does not vanish. Nevertheless, the glacial effect on SPEI shows strong variation across basins and across GCMs, suggesting considerable structural uncertainty. More fundamental work on the modelling of hydroclimate is thus clearly needed. Of greatest relevance to hydroclimate in glaciated basins will be the inclusion of online glacier models, increasing model resolution and associated improvements in the representation of hydroclimate-topography interactions, and improved simulation of frozen precipitation processes.

Acknowledgments

Monthly glacial water runoff model results were kindly provided by Matthias Huss. Readers are encouraged to reproduce the analysis for any basin of their choice using the code, data, and Jupyter notebook guide we have made available at `http://github.com/ehultee/glacial-SPEI`. This manuscript is SOEST publication number [XXXXX - *number will be provided if accepted and must be added to final version*].

References

Aizen, V. B., Aizen, E. M., & Nikitin, S. A. (2002). Glacier regime on the northern slope of the Himalaya (Xixibangma glaciers). *Quaternary International*, *97-98*, 27–39. doi: 10.1016/S1040-6182(02)00049-6

Allen, R. G., Pereira, L. S., Raes, D., & Smith, M. (1998). Crop evapotranspiration—guidelines for computing crop water requirements. In *FAO Irrigation and drainage paper* (Vol. 56). United Nations Food and Agriculture Organization.

Ault, T. R. (2020). On the essentials of drought in a changing climate. *Science*, *368*(6488), 256–260. doi: 10.1126/science.aaz5492

Barnett, T. P., Adam, J. C., & Lettenmaier, D. P. (2005). Potential impacts of a warming climate on water availability in snow-dominated regions. *Nature*, *438*(7066), 303–309. doi: 10.1038/nature04141

Biemans, H., Siderius, C., Lutz, A. F., Nepal, S., Ahmad, B., Hassan, T., ... Immerzeel, W. W. (2019). Importance of snow and glacier meltwater for agriculture on the Indo-Gangetic Plain. *Nature Sustainability*, *2*(7), 594–601. doi: 10.1038/s41893-019-0305-3

Bliss, A., Hock, R., & Radić, V. (2014). Global response of glacier runoff to twenty-first century climate change. *Journal of Geophysical Research: Earth Surface*, *119*(4), 717–730. doi: 10.1002/2013JF002931

Brunner, M. I., Farinotti, D., Zekollari, H., Huss, M., & Zappa, M. (2019). Future shifts in extreme flow regimes in Alpine regions. *Hydrology and Earth System Sciences*, *23*(11), 4471–4489. doi: 10.5194/hess-23-4471-2019

Cáceres, D., Marzeion, B., Malles, J. H., Gutknecht, B., Müller Schmied, H., & Döll, P. (2020). Assessing global water mass transfers from continents to oceans over the period 1948–2016. *Hydrology and Earth System Sciences Discussions*, *2020*, 1–37. doi: 10.5194/hess-2019-664

Carey, M., Molden, O. C., Rasmussen, M. B., Jackson, M., Nolin, A. W., & Mark, B. G. (2017). Impacts of glacier recession and declining meltwater on mountain societies. *Annals of the American Association of Geographers*, *107*(2), 350–359. doi: 10.1080/24694452.2016.1243039

Chidichimo, F., Mendoza, B. T., De Biase, M., Catelan, P., Straface, S., & Di Gregorio, S. (2018). Hydrogeological modeling of the groundwater recharge feeding the Chambo aquifer, Ecuador. *AIP Conference Proceedings*, *2022*(1), 020003. doi: 10.1063/1.5060683

Cook, B. I., Mankin, J. S., Marvel, K., Williams, A. P., Smerdon, J. E., & Anchukaitis, K. J. (2020). Twenty-first century drought projections in the CMIP6 forcing scenarios. *Earth's Future*, e2019EF001461. doi: 10.1029/2019EF001461

Cook, B. I., Smerdon, J. E., Seager, R., & Coats, S. (2014). Global warming and 21st century drying. *Climate Dynamics*, *43*(9-10), 2607–2627. doi: 10.1007/s00382-014-2075-y

Decharme, B., Delire, C., Minvielle, M., Colin, J., Vergnes, J.-P., Alias, A., ... Voldoire, A. (2019). Recent changes in the ISBA-CTRIP land surface system for use in the CNRM-CM6 climate model and in global off-line hydrological applications. *Journal of Advances in Modeling Earth Systems*, *11*(5), 1207–1252. doi: 10.1029/2018MS001545

Dee, D. P., Uppala, S. M., Simmons, A. J., Berrisford, P., Poli, P., Kobayashi, S., ... Vitart, F. (2011). The ERA-Interim reanalysis: configuration and performance of the data assimilation system. *Quarterly Journal of the Royal Meteorological Society*, *137*(656), 553–597. doi: 10.1002/qj.828

de Kok, R. J., Tuinenburg, O. A., Bonekamp, P. N. J., & Immerzeel, W. W. (2018, 2019/12/03). Irrigation as a potential driver for anomalous glacier behavior in High Mountain Asia. *Geophysical Research Letters*, *45*(4), 2047–2054. doi: 10.1002/2017GL076158

Flato, G., Marotzke, J., Abiodun, B., Braconnot, P., Chou, S., Collins, W., ... Rummukainen, M. (2013). Evaluation of climate models. In T. Stocker et al. (Eds.), *Climate change 2013: The physical science basis. Contribution of Working Group I to the Fifth Assessment Report of the Intergovernmental Panel on Climate Change.* Cambridge, United Kingdom and New York, NY, USA: Cambridge University Press.

Fleming, S. W., & Clarke, G. K. (2005). Attenuation of high-frequency interannual streamflow variability by watershed glacial cover. *Journal of Hydraulic Engineering*, *131*(7), 615–618. doi: 10.1061/(ASCE)0733-9429(2005)131:7(615)

Fountain, A. G., & Tangborn, W. V. (1985). The effect of glaciers on streamflow variations. *Water Resources Research*, *21*(4), 579–586. doi: 10.1029/

WR021i004p00579
Frans, C., Istanbulluoglu, E., Lettenmaier, D. P., Clarke, G., Bohn, T. J., & Stumbaugh, M. (2016). Implications of decadal to century scale glacio-hydrological change for water resources of the Hood River basin, OR, USA. *Hydrological Processes*, *30*(23), 4314-4329. doi: 10.1002/hyp.10872
Gagliardini, O., Zwinger, T., Gillet-Chaulet, F., Durand, G., Favier, L., Fleurian, B. d., ... Råback, P. (2013). Capabilities and performance of Elmer/Ice, a new-generation ice sheet model. *Geoscientific Model Development*, *6*(4), 1299–1318. doi: 10.5194/gmdd-6-1689-2013
Global Runoff Data Centre. (2007). *Major river basins of the world.* http://grdc.bafg.de. 56068 Koblenz, Germany.
Head, L., Atchison, J., Gates, A., & Muir, P. (2011). A fine-grained study of the experience of drought, risk and climate change among Australian wheat farming households. *Annals of the Association of American Geographers*, *101*(5), 1089–1108. doi: 10.1080/00045608.2011.579533
Huss, M., & Hock, R. (2018). Global-scale hydrological response to future glacier mass loss. *Nature Climate Change*, *8*(2), 135–140. doi: 10.1038/s41558-017-0049-x
Immerzeel, W. W., Lutz, A. F., Andrade, M., Bahl, A., Biemans, H., Bolch, T., ... Baillie, J. E. M. (2020). Importance and vulnerability of the world's water towers. *Nature*, *577*(7790), 364–369. doi: 10.1038/s41586-019-1822-y
Immerzeel, W. W., van Beek, L. P. H., & Bierkens, M. F. P. (2010). Climate change will affect the Asian water towers. *Science*, *328*(5984), 1382. doi: 10.1126/science.1183188
Immerzeel, W. W., van Beek, L. P. H., Konz, M., Shrestha, A. B., & Bierkens, M. F. P. (2012). Hydrological response to climate change in a glacierized catchment in the Himalayas. *Climatic Change*, *110*(3), 721–736. doi: 10.1007/s10584-011-0143-4
Jiang, P., Liu, H., Wu, X., & Wang, H. (2017). Tree-ring-based SPEI reconstruction in central Tianshan Mountains of China since A.D. 1820 and links to westerly circulation. *International Journal of Climatology*, *37*(6), 2863–2872. doi: 10.1002/joc.4884
Juen, I., Kaser, G., & Georges, C. (2007). Modelling observed and future runoff from a glacierized tropical catchment (Cordillera Blanca, Perú). *Global and Planetary Change*, *59*(1), 37–48. doi: https://doi.org/10.1016/j.gloplacha.2006.11.038
Kaser, G., Großhauser, M., & Marzeion, B. (2010). Contribution potential of glaciers to water availability in different climate regimes. *Proceedings of the National Academy of Sciences*, *107*(47), 20223–20227. doi: 10.1073/pnas.1008162107
Kingston, D. G., Stagge, J. H., Tallaksen, L. M., & Hannah, D. M. (2014). European-scale drought: Understanding connections between atmospheric circulation and meteorological drought indices. *Journal of Climate*, *28*(2), 505–516. doi: 10.1175/JCLI-D-14-00001.1
Lawrence, D., Fisher, R., Koven, C., Oleson, K., Swenson, S., & Vertenstein, M. (2018). *Technical description of version 5.0 of the Community Land Model (CLM)* (Tech. Rep.). National Center for Atmospheric Research.
Leblanc, M. J., Tregoning, P., Ramillien, G., Tweed, S. O., & Fakes, A. (2009). Basin-scale, integrated observations of the early 21st century multiyear drought in southeast australia. *Water Resources Research*, *45*(4).
Lehner, F., Wood, A. W., Vano, J. A., Lawrence, D. M., Clark, M. P., & Mankin, J. S. (2019). The potential to reduce uncertainty in regional runoff projections from climate models. *Nature Climate Change*, *9*(12), 926–933.
Liljedahl, A. K., Gädeke, A., O'Neel, S., Gatesman, T. A., & Douglas, T. A. (2017). Glacierized headwater streams as aquifer recharge corridors, subarctic Alaska. *Geophysical Research Letters*, *44*(13), 6876–6885. doi:

10.1002/2017GL073834
Lorenzo-Lacruz, J., Vicente-Serrano, S. M., López-Moreno, J. I., Beguería, S., García-Ruiz, J. M., & Cuadrat, J. M. (2010). The impact of droughts and water management on various hydrological systems in the headwaters of the Tagus River (central Spain). *Journal of Hydrology*, *386*(1), 13–26. doi: 10.1016/j.jhydrol.2010.01.001
Mackay, J. D., Barrand, N. E., Hannah, D. M., Krause, S., Jackson, C. R., Everest, J., ... Black, A. R. (2019). Future evolution and uncertainty of river flow regime change in a deglaciating river basin. *Hydrology and Earth System Sciences*, *23*(4), 1833–1865. doi: 10.5194/hess-23-1833-2019
Mankin, J. S., Seager, R., Smerdon, J. E., Cook, B. I., & Williams, A. P. (2019). Mid-latitude freshwater availability reduced by projected vegetation responses to climate change. *Nature Geoscience*, 1–6. doi: 10.1038/s41561-019-0480-x
Mankin, J. S., Seager, R., Smerdon, J. E., Cook, B. I., Williams, A. P., & Horton, R. M. (2018). Blue water trade-offs with vegetation in a CO2-enriched climate. *Geophysical Research Letters*, *45*(7), 3115–3125. doi: 10.1002/2018GL077051
Mankin, J. S., Smerdon, J. E., Cook, B. I., Williams, A. P., & Seager, R. (2017). The curious case of projected twenty-first-century drying but greening in the American West. *Journal of Climate*, *30*(21), 8689–8710. doi: 10.1175/JCLI-D-17-0213.1
Marzeion, B., Hock, R., Anderson, B., Bliss, A., Champollion, N., Fujita, K., ... Zekollari, H. (2020). Partitioning the uncertainty of ensemble projections of global glacier mass change. *Earth's Future*, e2019EF001470. doi: 10.1029/2019EF001470
Marzeion, B., Kaser, G., Maussion, F., & Champollion, N. (2018). Limited influence of climate change mitigation on short-term glacier mass loss. *Nature Climate Change*, *8*(4), 305–308. doi: 10.1038/s41558-018-0093-1
Maussion, F., Butenko, A., Champollion, N., Dusch, M., Eis, J., Fourteau, K., ... Marzeion, B. (2019). The Open Global Glacier Model (OGGM) v1.1. *Geoscientific Model Development*, *12*(3), 909–931. doi: 10.5194/gmd-12-909-2019
McEvoy, D. J., Huntington, J. L., Abatzoglou, J. T., & Edwards, L. M. (2012). An evaluation of multiscalar drought indices in Nevada and Eastern California. *Earth Interactions*, *16*(18), 1–18.
McKee, T. B., Doesken, N. J., & Kleist, J. (1993). The relationship of drought frequency and duration to time scales. In *Proceedings of the 8th Conference on Applied Climatology, 17-22 January 1993, Anaheim, CA.* Boston, MA.
Milly, P. C., Betancourt, J., Falkenmark, M., Hirsch, R. M., Kundzewicz, Z. W., Lettenmaier, D. P., & Stouffer, R. J. (2008). Stationarity is dead: Whither water management? *Science*, *319*(5863), 573. doi: 10.1126/science.1151915
Milly, P. C., & Dunne, K. A. (2016). Potential evapotranspiration and continental drying. *Nature Climate Change*, *6*(10), 946. doi: 10.1038/nclimate3046
Noël, B., van de Berg, W., van Meijgaard, E., Munneke, P. K., van de Wal, R., & van den Broeke, M. (2015). Evaluation of the updated regional climate model RACMO2.3: summer snowfall impact on the Greenland Ice Sheet. *The Cryosphere*, *9*, 1831-1844. doi: 10.5194/tc-9-1831-2015
Obleitner, F. (1994). Climatological features of glacier and valley winds at the Hintereisferner (Ötztal Alps, Austria). *Theoretical and Applied Climatology*, *49*(4), 225–239. doi: 10.1007/BF00867462
Palmer, W. C. (1965). *Meteorological drought* (Tech. Rep. No. Research Paper No. 45). Washington, DC: US Weather Bureau.
Potop, V., Možný, M., & Soukup, J. (2012). Drought evolution at various time scales in the lowland regions and their impact on vegetable crops in the Czech Republic. *Agricultural and Forest Meteorology*, *156*, 121–133. doi: 10.1016/j.agrformet.2012.01.002
Pritchard, H. D. (2019). Asia's shrinking glaciers protect large populations from

drought stress. *Nature*, *569*(7758), 649–654. doi: 10.1038/s41586-019-1240-1

Rounce, D. R., Hock, R., & Shean, D. E. (2020). Glacier mass change in High Mountain Asia through 2100 using the open-source Python Glacier Evolution Model (PyGEM). *Frontiers in Earth Science*, *7*, 331. doi: 10.3389/feart.2019.00331

Rowan, A. V., Quincey, D. J., Gibson, M. J., Glasser, N. F., Westoby, M. J., Irvine-Fynn, T. D. L., . . . Hambrey, M. J. (2018). The sustainability of water resources in High Mountain Asia in the context of recent and future glacier change. *Geological Society, London, Special Publications*, *462*(1), 189. doi: 10.1144/SP462.12

Schaefli, B., Manso, P., Fischer, M., Huss, M., & Farinotti, D. (2019). The role of glacier retreat for Swiss hydropower production. *Renewable Energy*, *132*, 615–627. doi: 10.1016/j.renene.2018.07.104

Scheff, J., Seager, R., Liu, H., & Coats, S. (2017). Are glacials dry? Consequences for paleoclimatology and for greenhouse warming. *Journal of Climate*, *30*(17), 6593–6609. doi: 10.1175/JCLI-D-16-0854.1

Skamarock, W. C., Klemp, J. B., Dudhia, J., Gill, D. O., Liu, Z., Berner, J., . . . Huang, X.-Y. (2019). *A description of the Advanced Research WRF version 4.* NCAR Tech. Note NCAR/TN-556+STR. doi: 10.5065/1dfh-6p97

Somers, L. D., McKenzie, J. M., Mark, B. G., Lagos, P., Ng, G.-H. C., Wickert, A. D., . . . Silva, Y. (2019). Groundwater buffers decreasing glacier melt in an Andean watershed—but not forever. *Geophysical Research Letters*, *46*(22), 13016–13026. doi: 10.1029/2019GL084730

Sorg, A., Bolch, T., Stoffel, M., Solomina, O., & Beniston, M. (2012). Climate change impacts on glaciers and runoff in Tien Shan (Central Asia). *Nature Climate Change*, *2*(10), 725–731. doi: 10.1038/nclimate1592

Soruco, A., Vincent, C., Rabatel, A., Francou, B., Thibert, E., Sicart, J. E., & Condom, T. (2015). Contribution of glacier runoff to water resources of La Paz city, Bolivia (16 °S). *Annals of Glaciology*, *56*(70), 147-154. doi: 10.3189/2015AoG70A001

Swann, A. L., Hoffman, F. M., Koven, C. D., & Randerson, J. T. (2016). Plant responses to increasing CO2 reduce estimates of climate impacts on drought severity. *Proceedings of the National Academy of Sciences*, *113*(36), 10019–10024. doi: 10.1073/pnas.1604581113

Szalai, S., Szinell, C., & Zoboki, J. (2000). *Drought monitoring in Hungary* (Vol. 57; Tech. Rep.). Geneva, Switzerland: World Meteorological Organization.

Takata, K., Emori, S., & Watanabe, T. (2003). Development of the minimal advanced treatments of surface interaction and runoff. *Global and Planetary Change*, *38*(1), 209–222. doi: 10.1016/S0921-8181(03)00030-4

Taylor, K. E., Stouffer, R. J., & Meehl, G. A. (2011). An overview of CMIP5 and the experiment design. *Bulletin of the American Meteorological Society*, *93*(4), 485–498. doi: 10.1175/BAMS-D-11-00094.1

van den Broeke, M. R. (1997). Structure and diurnal variation of the atmospheric boundary layer over a mid-latitude glacier in summer. *Boundary-Layer Meteorology*, *83*(2), 183–205. doi: 10.1023/A:1000268825998

van de Wal, R. S. W., & Wild, M. (2001). Modelling the response of glaciers to climate change by applying volume-area scaling in combination with a high resolution GCM. *Climate Dynamics*, *18*(3), 359–366. doi: 10.1007/s003820100184

Vergara, W., Deeb, A., Valencia, A., Bradley, R., Francou, B., Zarzar, A., . . . Haeussling, S. (2007). Economic impacts of rapid glacier retreat in the Andes. *Eos, Transactions American Geophysical Union*, *88*(25), 261–264. doi: 10.1029/2007EO250001

Verseghy, D. L. (2000). The Canadian land surface scheme (CLASS): Its history and future. *Atmosphere-Ocean*, *38*(1), 1–13. doi: 10.1080/07055900.2000.9649637

Vicente-Serrano, S. M., Beguería, S., & López-Moreno, J. I. (2009). A multiscalar drought index sensitive to global warming: The standardized precipitation evapotranspiration index. *Journal of Climate*, *23*(7), 1696–1718. doi: 10.1175/2009JCLI2909.1

Vicente-Serrano, S. M., & López-Moreno, J. I. (2005). Hydrological response to different time scales of climatological drought: an evaluation of the Standardized Precipitation Index in a mountainous Mediterranean basin. *Hydrology and Earth System Sciences*, *9*(5), 523–533. doi: 10.5194/hess-9-523-2005

Vincent, A., Violette, S., & Aalgeirsdóttir, G. (2019). Groundwater in catchments headed by temperate glaciers: A review. *Earth-Science Reviews*, *188*, 59–76. doi: 10.1016/j.earscirev.2018.10.017

World Meteorological Organization, & Global Water Partnership. (2016). *Handbook of drought indicators and indices* (Tech. Rep.). Geneva, Switzerland: Integrated Drought Management Programme (IDMP).

Yang, Y., Roderick, M. L., Zhang, S., McVicar, T. R., & Donohue, R. J. (2019). Hydrologic implications of vegetation response to elevated CO2 in climate projections. *Nature Climate Change*, *9*(1), 44. doi: 10.1038/s41558-018-0361-0

Zhang, D., Zhang, Q., Werner, A. D., & Liu, X. (2016). GRACE-based hydrological drought evaluation of the Yangtze River Basin, China. *Journal of Hydrometeorology*, *17*(3), 811–828. doi: 10.1175/JHM-D-15-0084.1

S2. Glacial effect on 30-yr running mean SPEI by basin

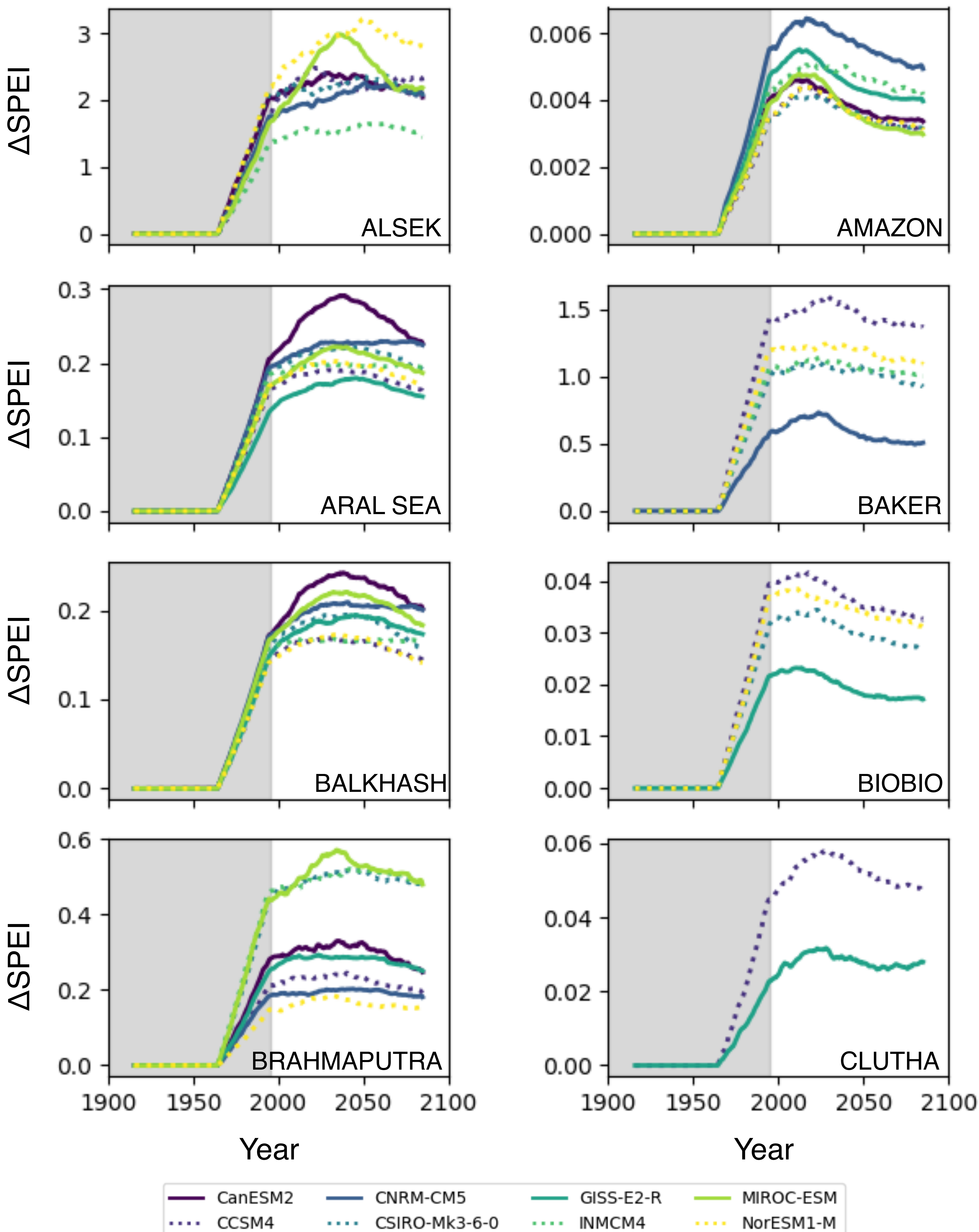

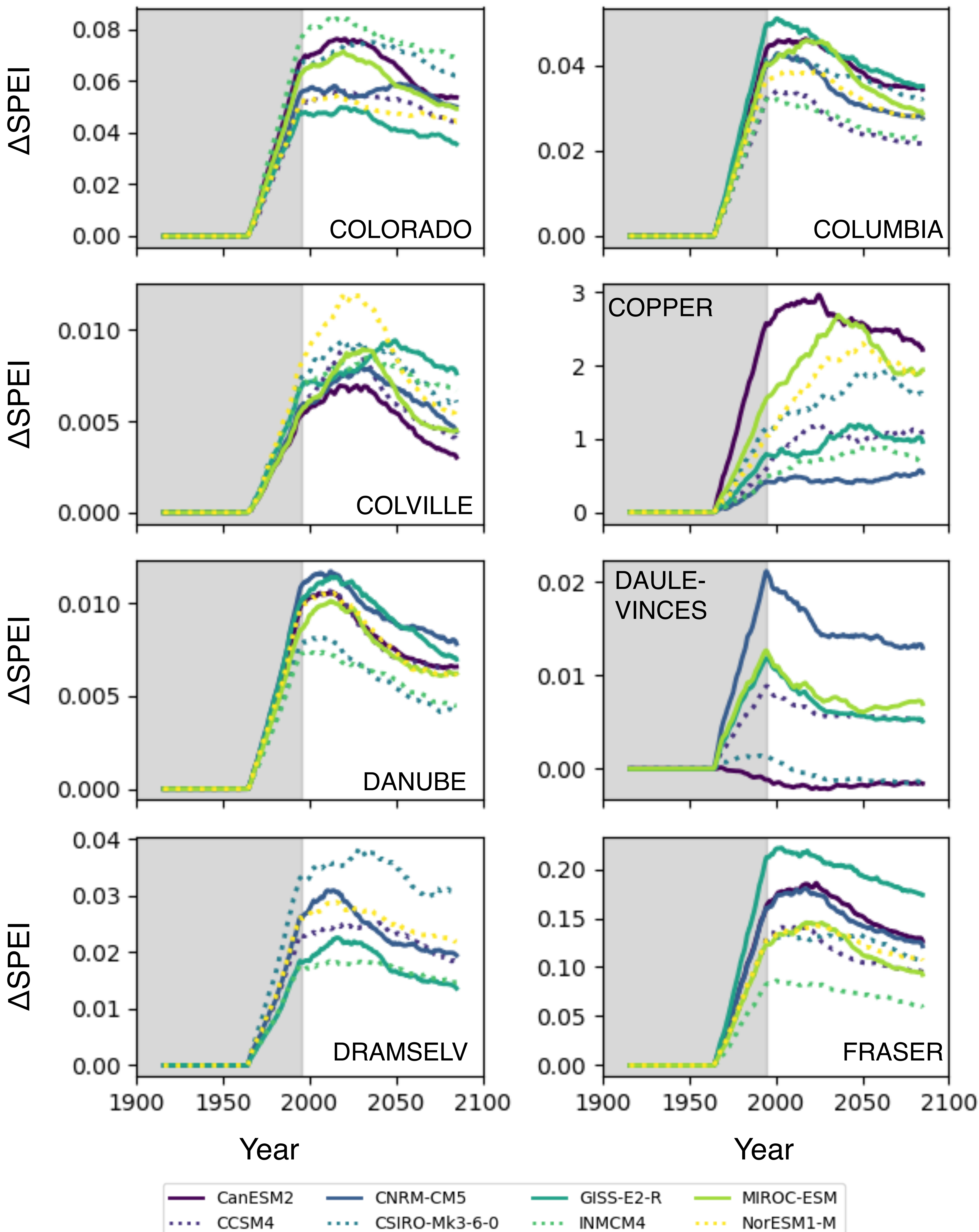

ΔSPEI
COLORADO
COLUMBIA
COLVILLE
COPPER
DANUBE
DAULE-
VINCES
DRAMSELV
FRASER
Year
CanESM2
CNRM-CM5
GISS-E2-R
MIROC-ESM
CCSM4
CSIRO-Mk3-6-0
INMCM4
NorESM1-M

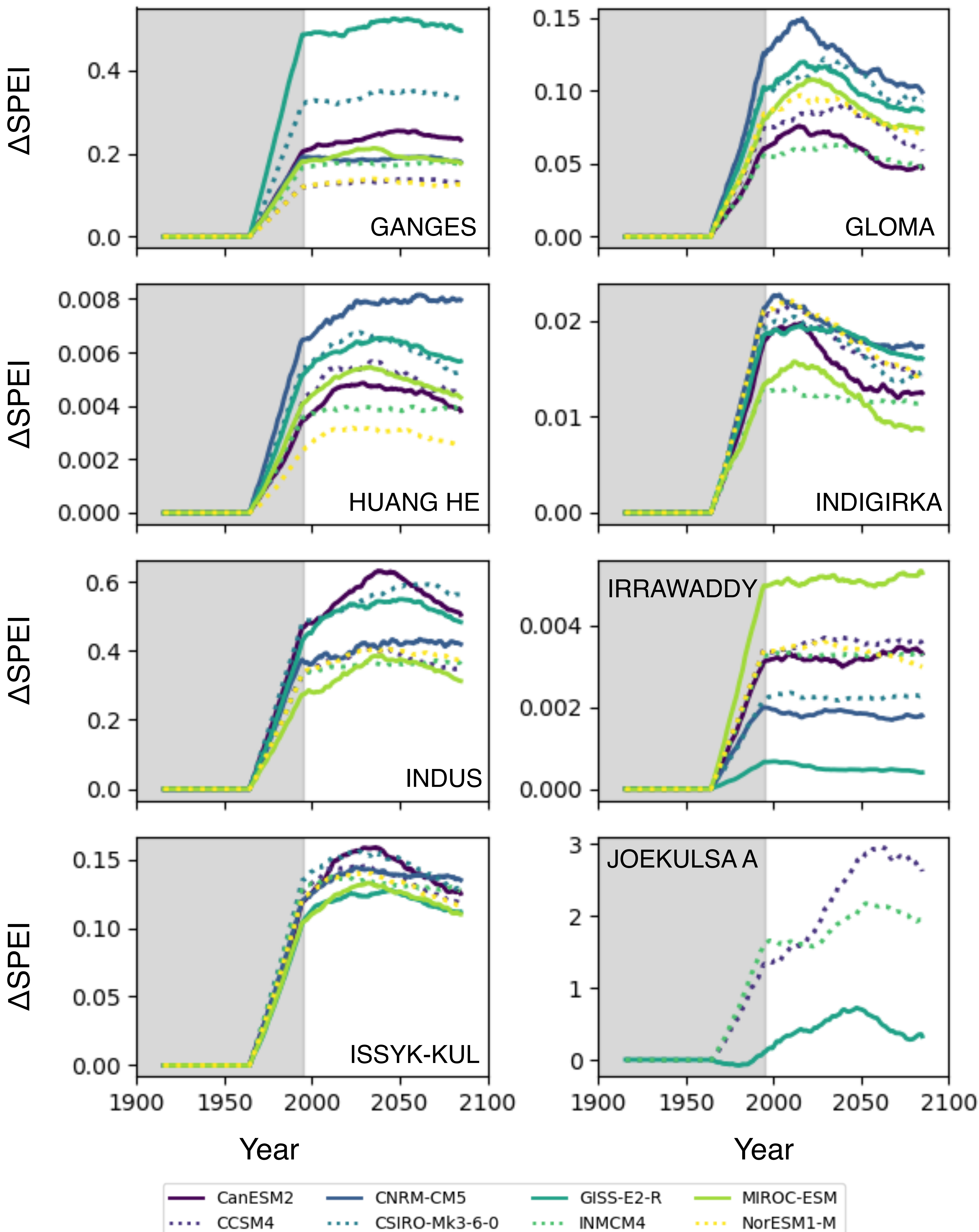

ΔSPEI
GANGES
GLOMA
HUANG HE
INDIGIRKA
INDUS
IRRAWADDY
ISSYK-KUL
JOEKULSA A
Year
CanESM2
CNRM-CM5
GISS-E2-R
MIROC-ESM
CCSM4
CSIRO-Mk3-6-0
INMCM4
NorESM1-M

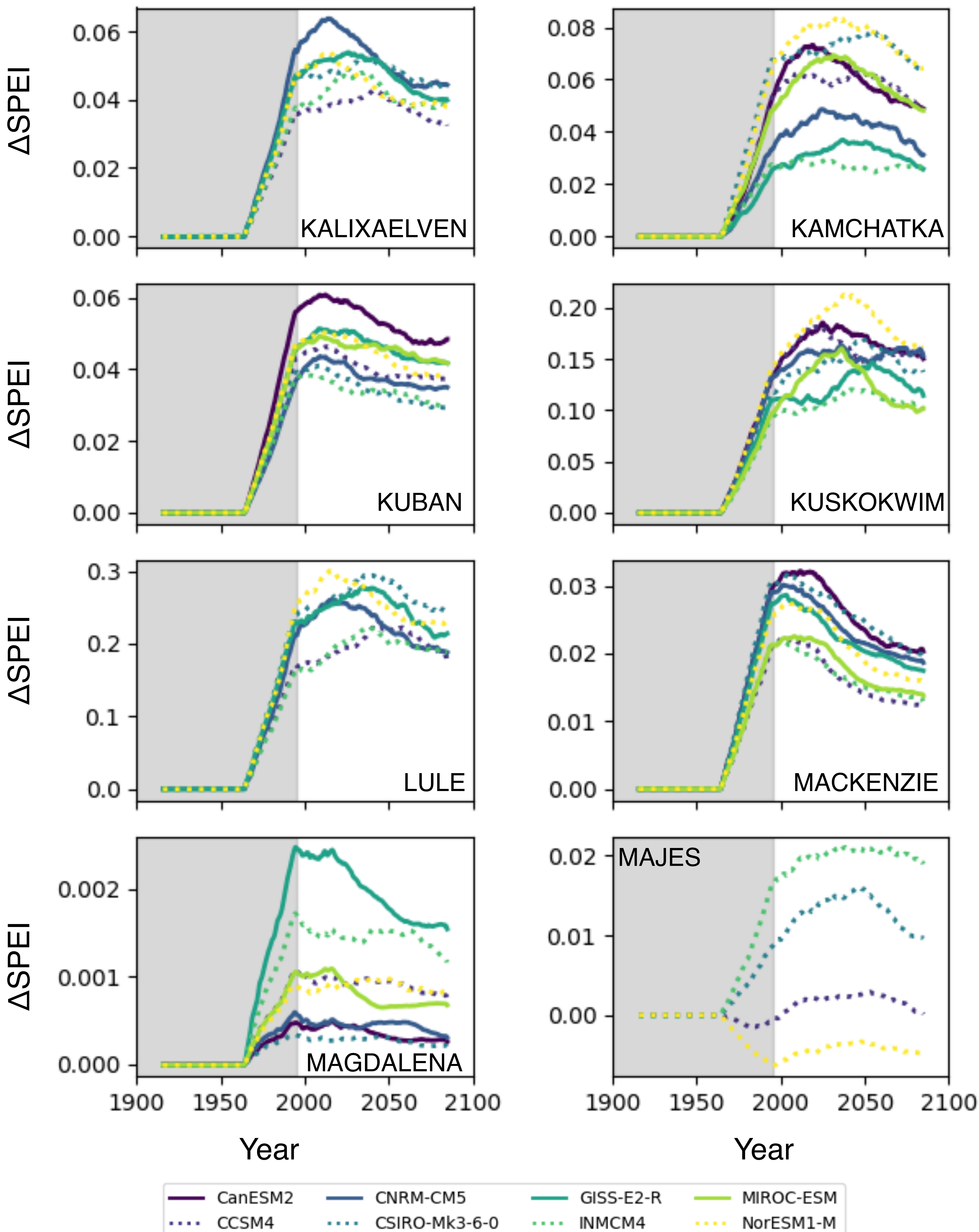

ΔSPEI
Year
KALIXAELVEN
KAMCHATKA
KUBAN
KUSKOKWIM
LULE
MACKENZIE
MAGDALENA
MAJES
CanESM2
CNRM-CM5
GISS-E2-R
MIROC-ESM
CCSM4
CSIRO-Mk3-6-0
INMCM4
NorESM1-M

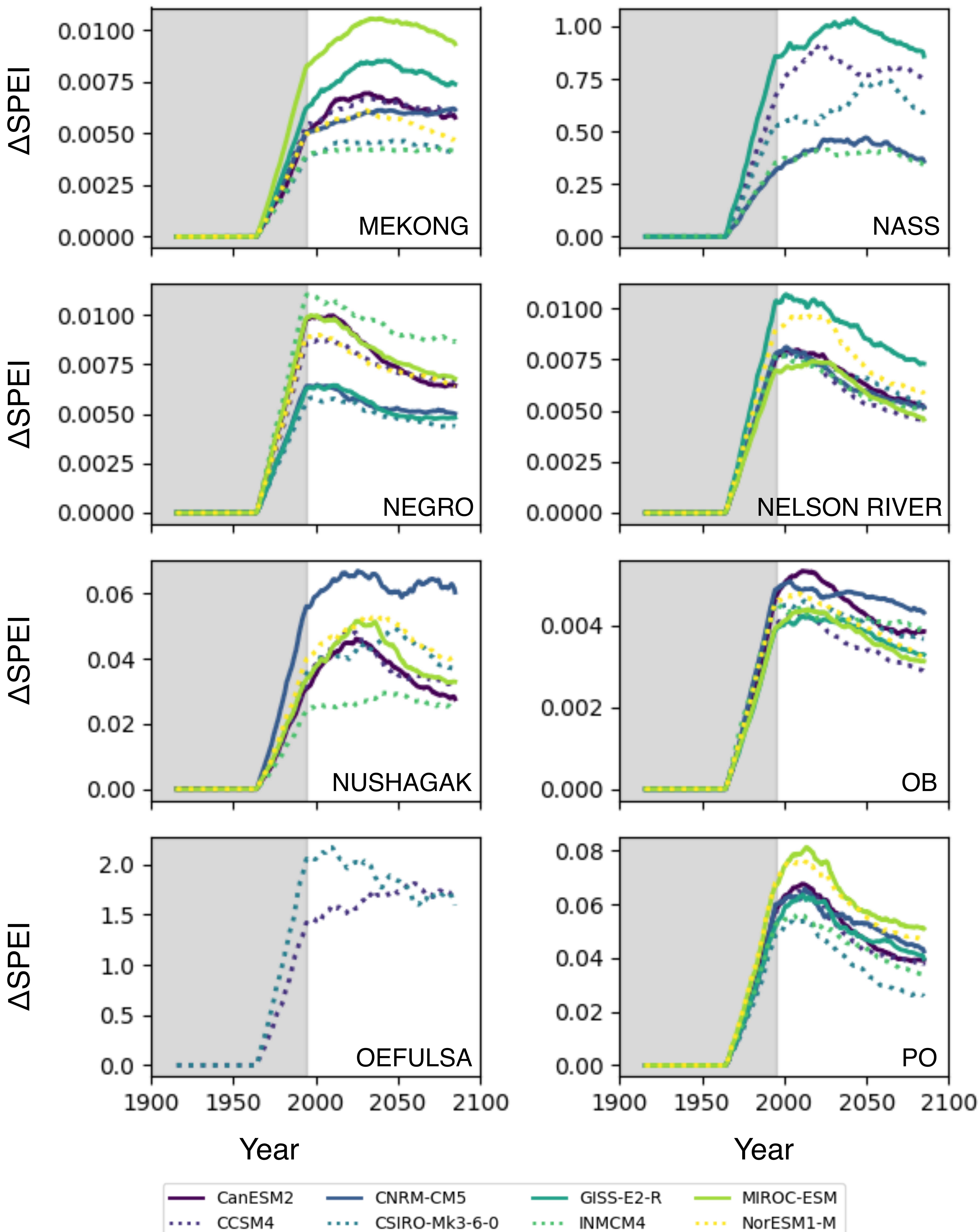

ΔSPEI
Year
MEKONG
NASS
NEGRO
NELSON RIVER
NUSHAGAK
OB
OEFULSA
PO
CanESM2
CCSM4
CNRM-CM5
CSIRO-Mk3-6-0
GISS-E2-R
INMCM4
MIROC-ESM
NorESM1-M

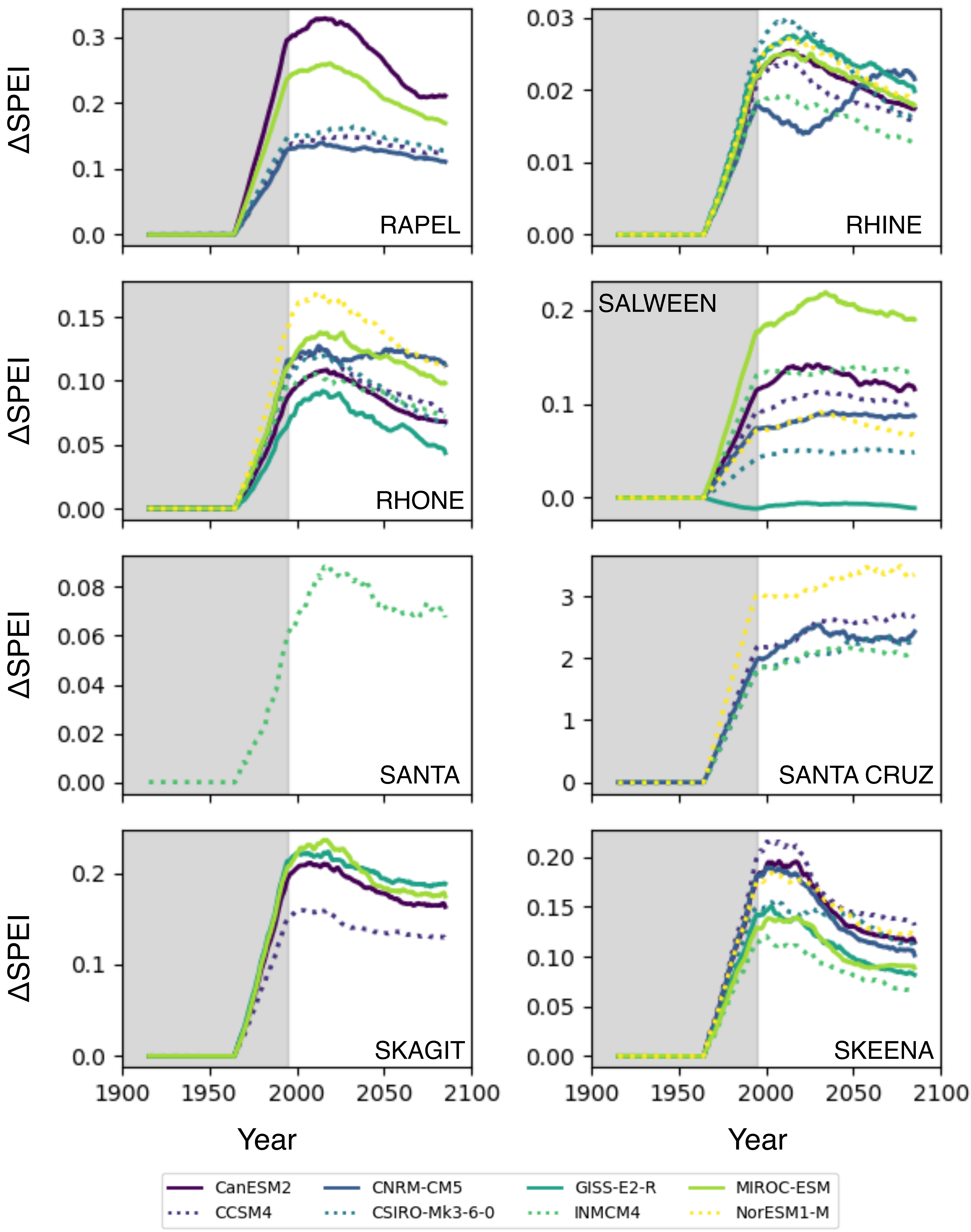
RAPEL
RHINE
RHONE
SALWEEN
SANTA
SANTA CRUZ
SKAGIT
SKEENA
ΔSPEI
Year
CanESM2
CCSM4
CNRM-CM5
CSIRO-Mk3-6-0
GISS-E2-R
INMCM4
MIROC-ESM
NorESM1-M

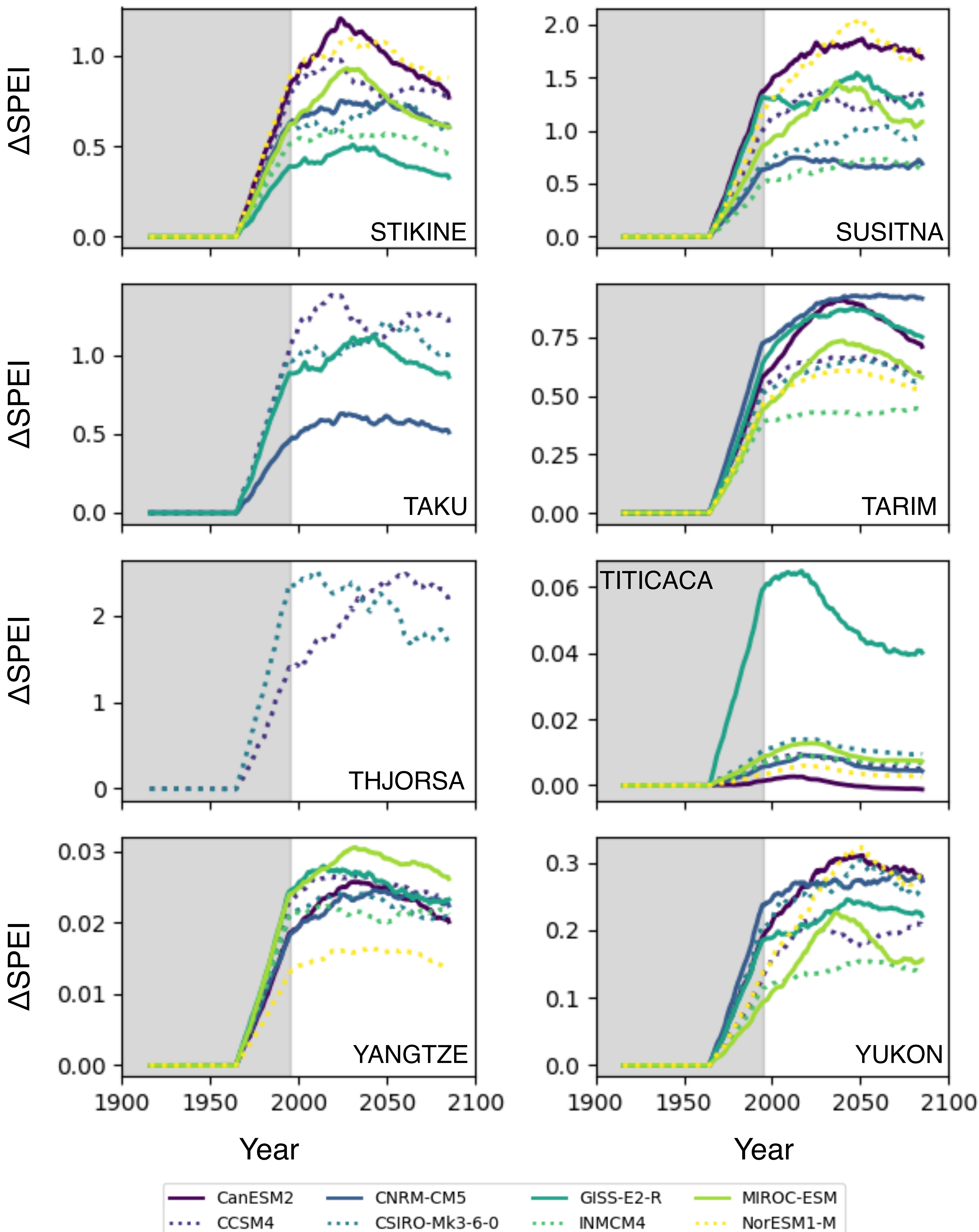
ΔSPEI
STIKINE
SUSITNA
TAKU
TARIM
THJORSA
TITICACA
YANGTZE
YUKON
Year
CanESM2
CCSM4
CNRM-CM5
CSIRO-Mk3-6-0
GISS-E2-R
INMCM4
MIROC-ESM
NorESM1-M

S3. Glacial effect on 30-yr running SPEI variance by basin

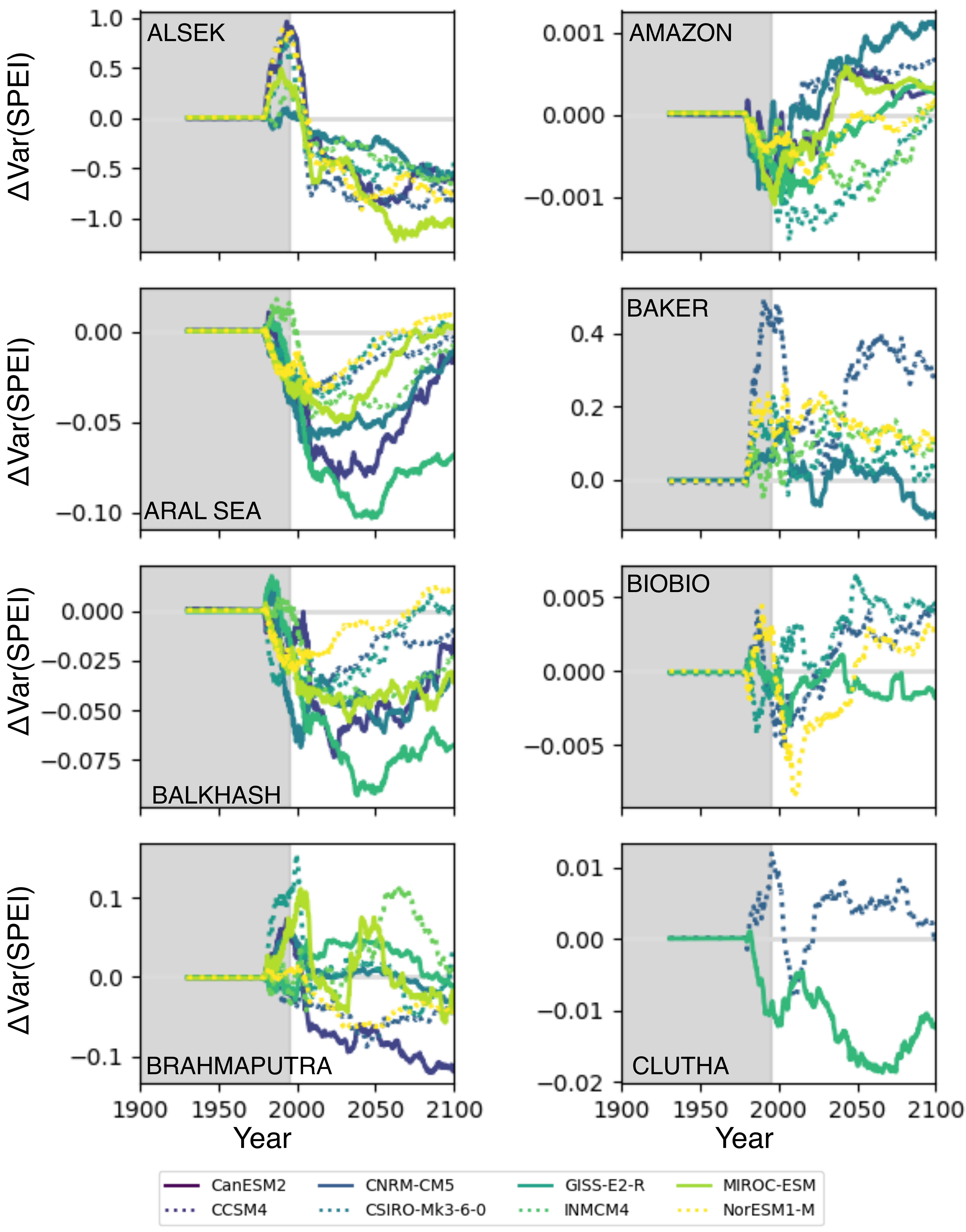

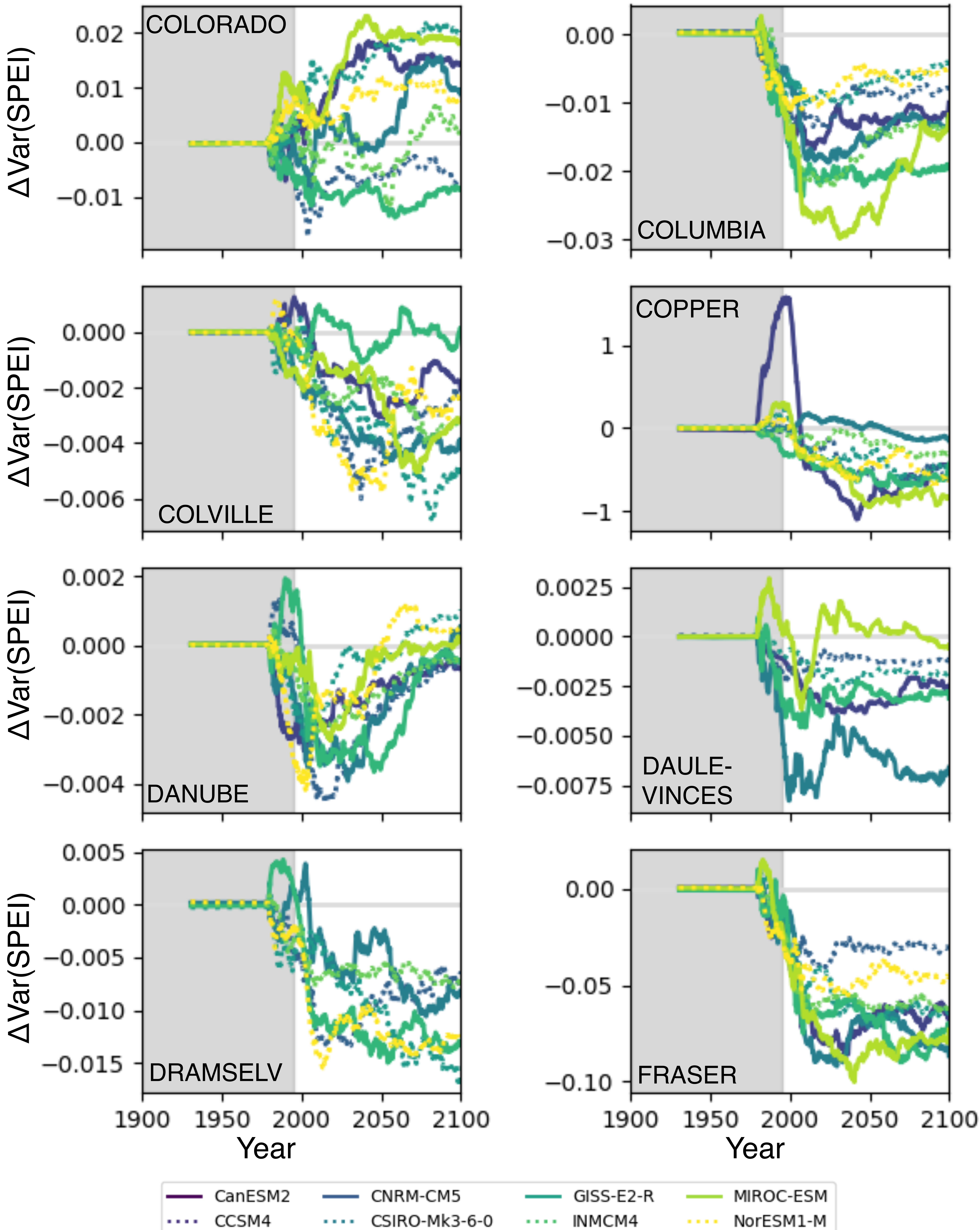

COLORADO
COLUMBIA
COLVILLE
COPPER
DANUBE
DAULE-VINCES
DRAMSELV
FRASER
ΔVar(SPEI)
Year
1900
1950
2000
2050
2100
CanESM2
CCSM4
CNRM-CM5
CSIRO-Mk3-6-0
GISS-E2-R
INMCM4
MIROC-ESM
NorESM1-M

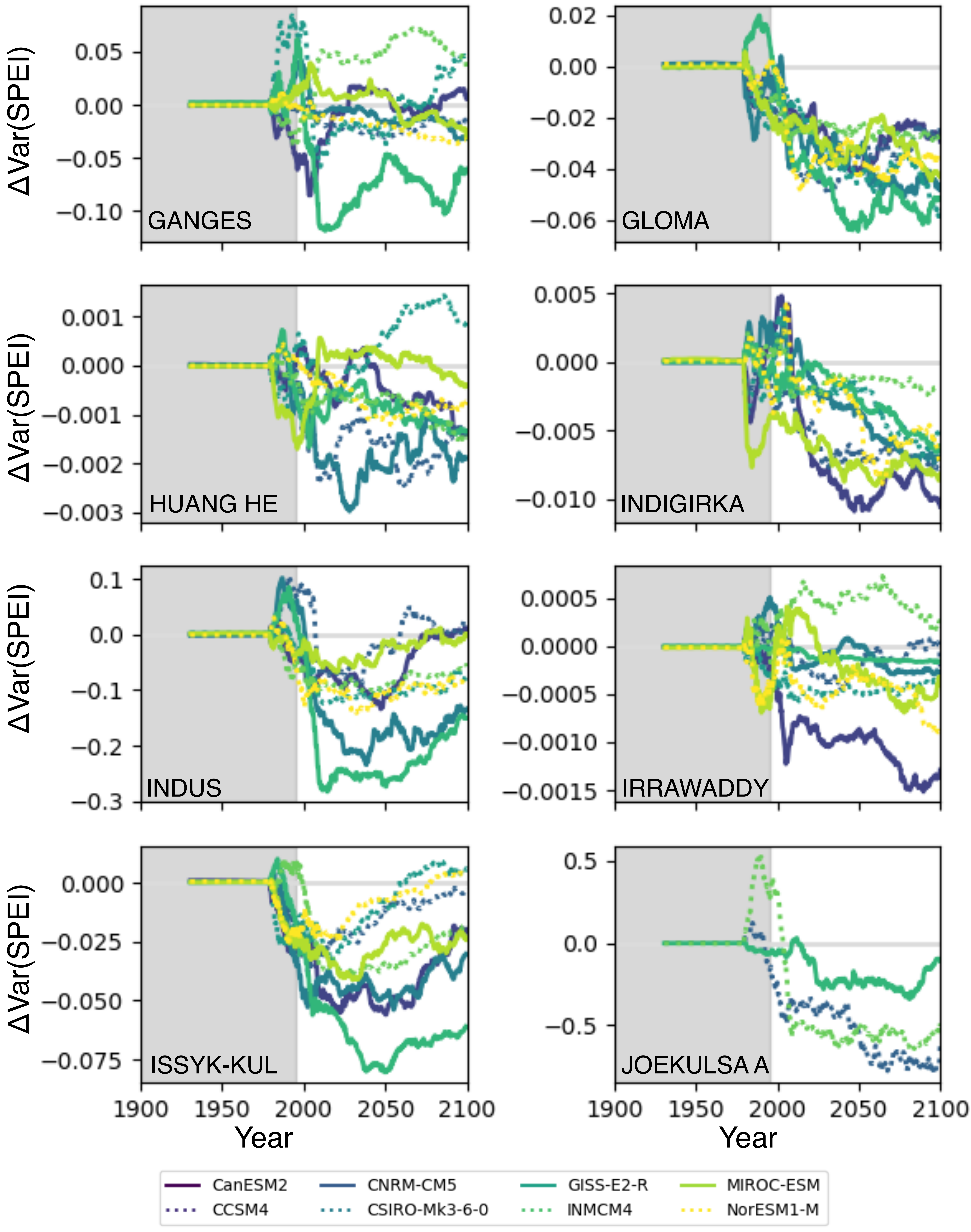
GANGES
GLOMA
HUANG HE
INDIGIRKA
INDUS
IRRAWADDY
ISSYK-KUL
JOEKULSA A
ΔVar(SPEI)
Year
1900
1950
2000
2050
2100
CanESM2
CCSM4
CNRM-CM5
CSIRO-Mk3-6-0
GISS-E2-R
INMCM4
MIROC-ESM
NorESM1-M

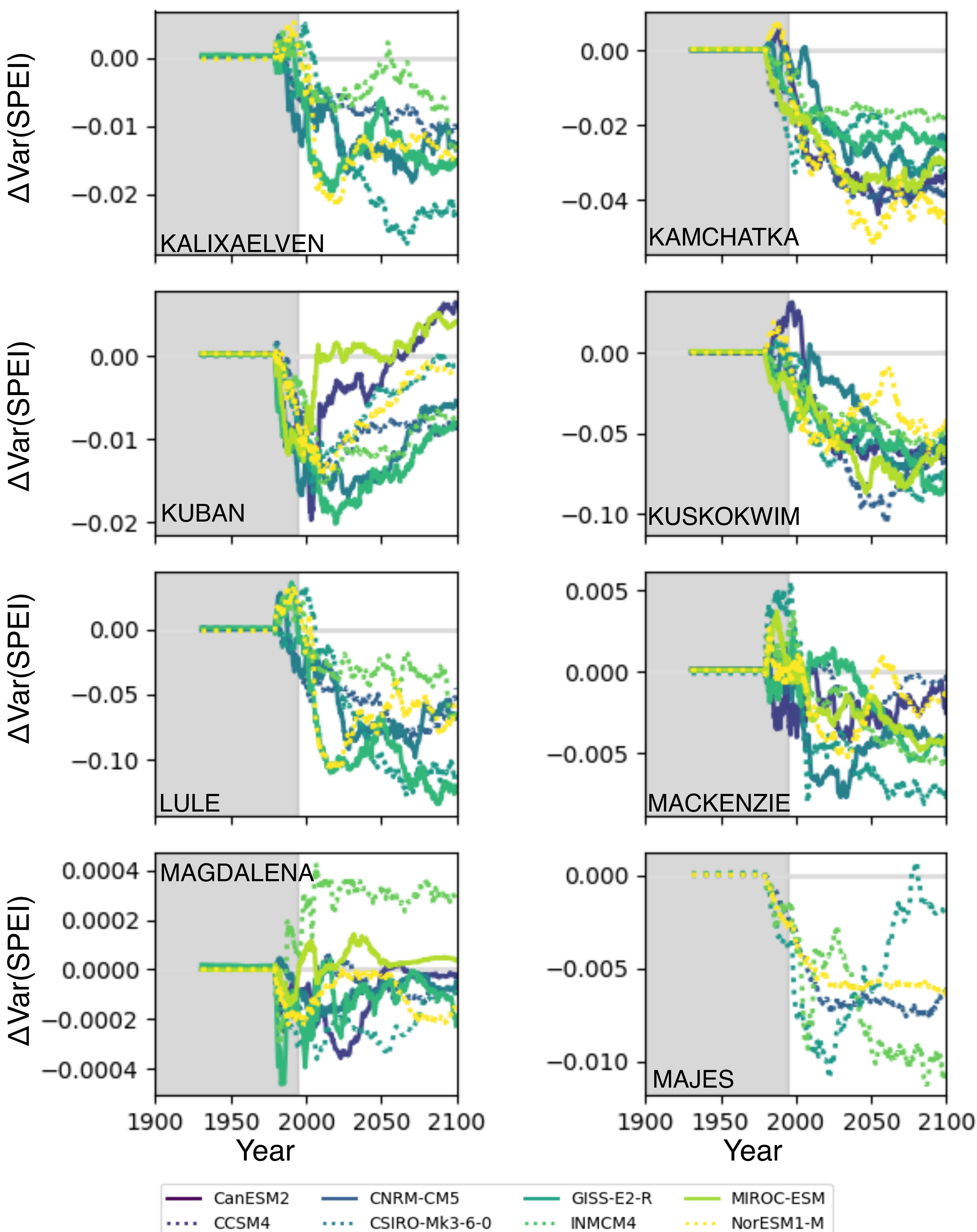

ΔVar(SPEI)
KALIXAELVEN
KAMCHATKA
KUBAN
KUSKOKWIM
LULE
MACKENZIE
MAGDALENA
MAJES
Year
CanESM2
CNRM-CM5
GISS-E2-R
MIROC-ESM
CCSM4
CSIRO-Mk3-6-0
INMCM4
NorESM1-M

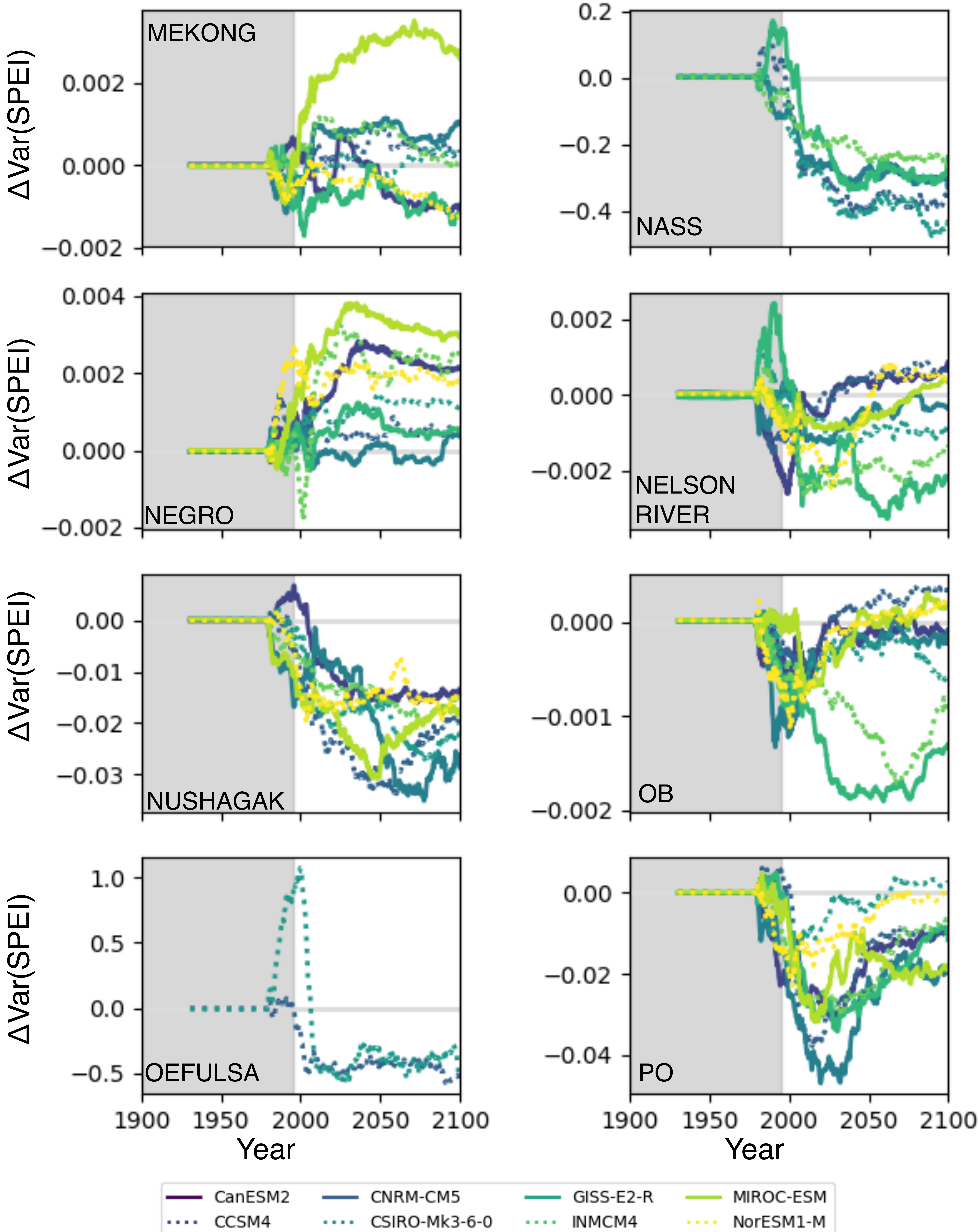
MEKONG
NASS
NEGRO
NELSON RIVER
NUSHAGAK
OB
OEFULSA
PO
ΔVar(SPEI)
Year
CanESM2
CCSM4
CNRM-CM5
CSIRO-Mk3-6-0
GISS-E2-R
INMCM4
MIROC-ESM
NorESM1-M

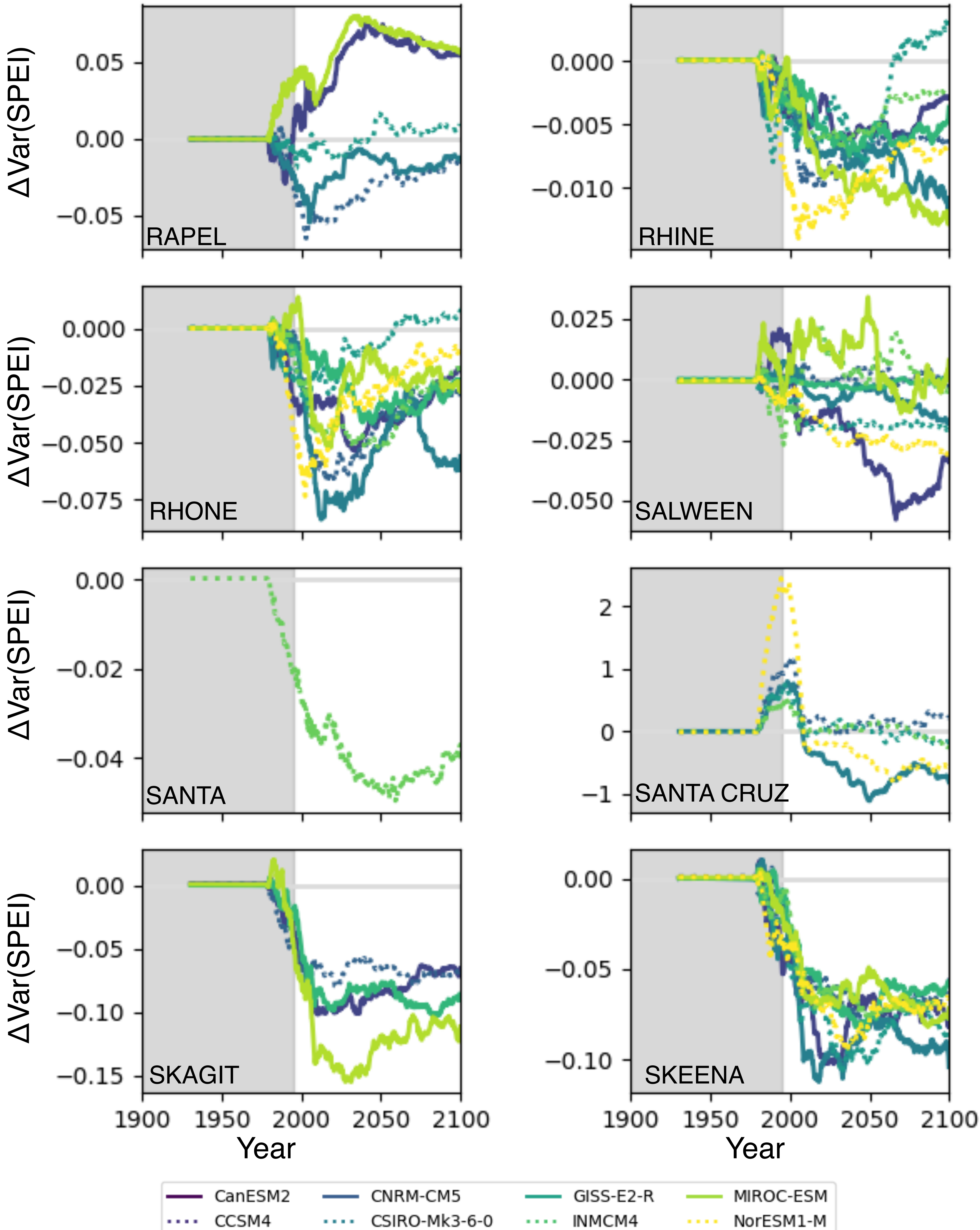
RAPEL
RHINE
RHONE
SALWEEN
SANTA
SANTA CRUZ
SKAGIT
SKEENA
ΔVar(SPEI)
Year
CanESM2
CCSM4
CNRM-CM5
CSIRO-Mk3-6-0
GISS-E2-R
INMCM4
MIROC-ESM
NorESM1-M

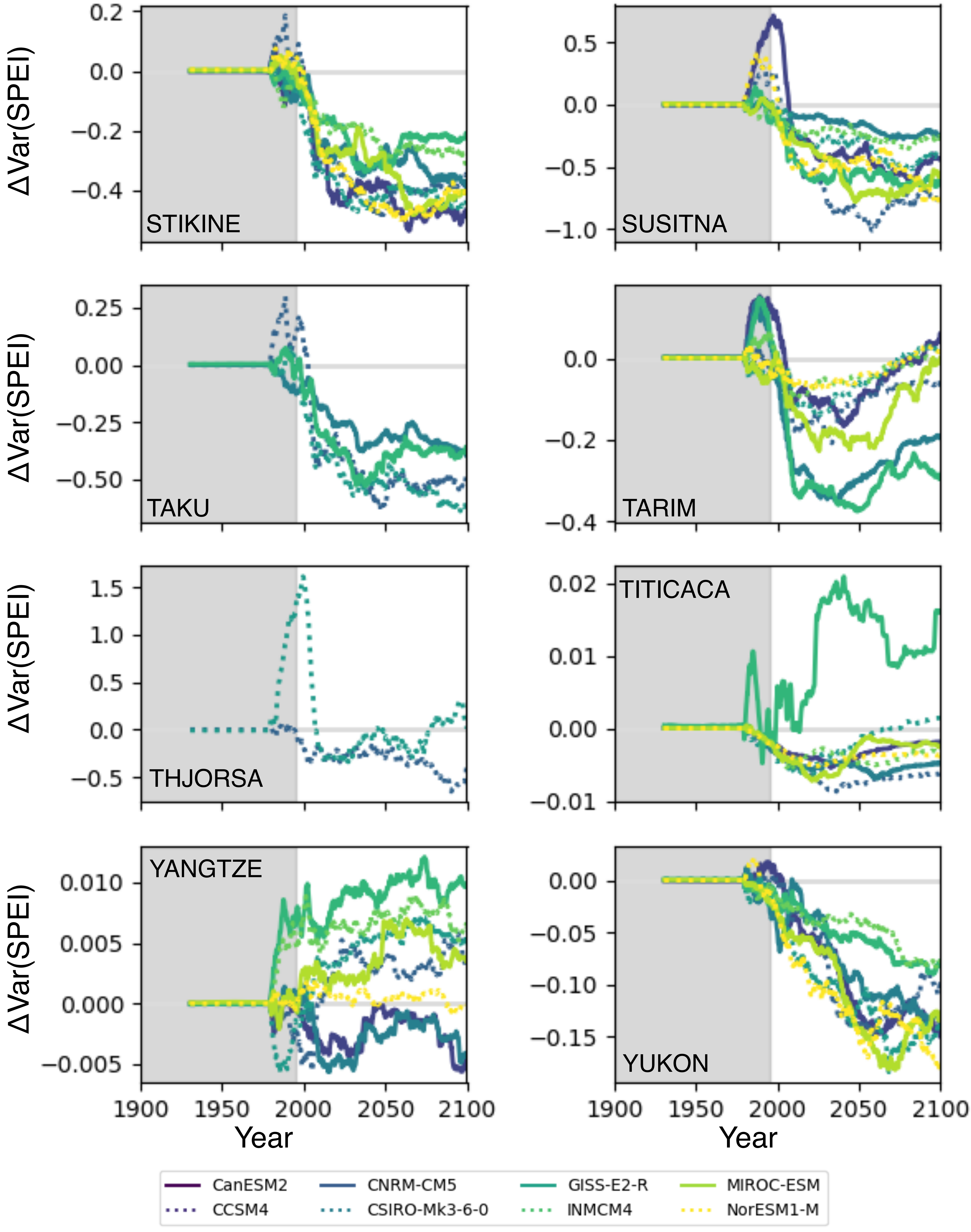

ΔVar(SPEI)
STIKINE
SUSITNA
TAKU
TARIM
THJORSA
TITICACA
YANGTZE
YUKON
Year
1900
1950
2000
2050
2100
CanESM2
CCSM4
CNRM-CM5
CSIRO-Mk3-6-0
GISS-E2-R
INMCM4
MIROC-ESM
NorESM1-M

Supporting Information for "Glacial runoff buffers drought through the 21st century—but models disagree on the details"

L. Ultee[1], S. Coats[2]

[1]Department of Earth, Atmospheric, and Planetary Sciences, Massachusetts Institute of Technology

[2]Department of Earth Sciences, University of Hawaii at Manoa

Contents of this file

1. Text S1 to S3
2. Captions to multi-panel figures S2 and S3
3. Figures S1 to S5

Introduction

All analysis shown in the main text is reproducible and extensible for any of the 56 basins using the Jupyter notebook and code we have provided on GitHub (see link in Acknowledgements). We encourage readers interested in detailed results for a specific basin to make use of the material provided there. The public code also allows users

---

Corresponding author: L. Ultee, Department of Earth, Atmospheric, and Planetary Sciences, Massachusetts Institute of Technology, Cambridge, MA 02139 USA. (ehultee@umich.edu)

to change time scales of analysis—for example, presenting running means over 5-year rather than 30-year windows, or calculating SPEI at a 27-month rather than 15-month timescale—and examine SPEI under the RCP 8.5 rather than RCP 4.5 emissions scenario.

For readers' convenience, we include below extended results for each of the 56 basins we analyzed, for the same time scales and climate scenario shown in the main text. The results are presented as multi-page sets of panels that replicate the panels shown in Figures 2 and 3 of the main text, but with all 56 basins rather than the 4 examples shown in the text. Figure S2 shows the glacial effect on mean SPEI. Figure S3 shows the glacial effect on SPEI variance. The panels in both figures were computed with climate scenario RCP 4.5, examining SPEI with a 15-month integration timescale, comparing statistics with a 30-year running window.

Text S1. SPEI computation

SPEI is computed by aggregating and normalizing a simple climatic water balance,

$$D_i = P_i - PET_i, \tag{S.1}$$

where P_i is the precipitation in time step i, PET_i is the potential evapotranspiration in the same time step, and D_i is their difference. We take precipitation P_i directly from the output of each GCM that we analyze, aggregated to basin scale as described in main text section 2. We estimate PET_i with the Penman-Montieth method, following Allen, Pereira, Raes, and Smith (1998). To calculate PET requires surface temperature, surface pressure, surface specific humidity, and surface net radiation from the GCM. Surface wind is set to be constant, as PET has been shown to be insensitive to the inclusion of surface wind from GCMs (Cook et al., 2014). All methods for calculating PET directly follow those in Cook et al. (2014).

Text S1.1. Sensitivity to integration timescale

SPEI includes a user-selected timescale of integration, which can be adjusted to study different types of drought and different parts of the hydroclimate system. Short timescales relate to availability of water as soil moisture and headwater river discharge, while longer timescales relate to reservoir storage, downstream water discharge, and changes in groundwater storage (Vicente-Serrano et al., 2009). In our analysis, we present SPEI computed with a relatively long integration timescale of 15 months. This choice reflects our focus on hydrological drought in semi-arid mountain basins dependent on frozen precipitation and seasonal snowmelt (see main text section 2 and McEvoy et al., 2012). We also computed SPEI at a range of integration timescales to ensure our results for the 15-month timescale were not anomalous. One example is below; results for all basins and timescales are available on our public repository.

Figure S1 shows the glacial effect on mean SPEI in the Tarim basin (compare with Figure 2b), with SPEI computed at seven different timescales of integration. The qualitative patterns of the glacial effect on SPEI are similar across integration timescales: some models show ΔSPEI increasing nearly monotonically, while others show an initial increase with a peak near midcentury and subsequent decline. Inter-GCM differences in ΔSPEI are broadly consistent across timescales, though the ordering of GCMs from smallest glacial effect in a basin to largest does vary. The magnitude of the glacial effect ranges from 0.1 SPEI units to 2 SPEI units at different timescales. Although the smallest-magnitude effect appears at the shortest timescale of integration in the Tarim basin, there is no monotonic relationship between ΔSPEI magnitude and integration timescale. That is, the magnitude of the effect we analyse does not scale linearly with the SPEI timescale.

Text S1.2. Uncertainties in non-glacial components of SPEI

One of the strengths of SPEI for analysing drought under a future changed climate is that it accounts for changing atmospheric demand for moisture. This accounting is not possible with drought metrics that account solely for precipitation, such as the Standardized Precipitation Index (McKee et al., 1993; World Meteorological Organization & Global Water Partnership, 2016). However, the methods used to compute atmospheric demand for moisture, in the form of PET, are a source of uncertainty in SPEI and other PET-based drought metrics. For example, Milly and Dunne (2016) found that the Penman-Montieth method for computing PET overpredicts non-water-stressed evapotranspiration under future climate change. Yang, Roderick, Zhang, McVicar, and Donohue (2019) suggest a method to correct PET under future climate change by including a varying stomatal conductance term in the Penman-Montieth calculation.

We have focused here on the large glacial contribution to SPEI, and uncertainties in the non-glacial components are not central to our analysis. Nevertheless, to ensure our results were robust, we recomputed all SPEI timeseries following the corrected PET method of Yang et al. (2019). We then compared SPEI_N and the glacial effect $\mathrm{SPEI}_W - \mathrm{SPEI}_N$ (see Methods) for each basin computed with and without the correction. Figure S4 shows per-basin differences in each, normalized by the single-basin multi-model mean of each value to facilitate comparison across basins. We find that although the Yang et al. (2019) correction can make a large difference in SPEI_N for individual basins, with a maximum of 107% difference for a single basin (Figure S4a), in most cases the correction is inconsequential. The percent difference in the glacial effect, $\mathrm{SPEI}_W - \mathrm{SPEI}_N$, is an order of magnitude lower (Figure S4b). A mean of -0.07% difference and an absolute maximum of 0.6% difference in glacial effect due to the inclusion of the Yang et al. (2019) correction confirm that our use of the uncorrected Penman-Montieth method does not impact our analysis or results.

Text S2. Accounting for glacial runoff

We account for glacial runoff in each basin during the period 1980-2100 using the runoff simulations of Huss and Hock (2018). Their model is forced by monthly near-surface air temperature and precipitation from global climate reanalysis (Dee et al., 2011) and CMIP5 GCM projections (Taylor et al., 2011), downscaled to each individual glacier. The initial area of each glacier is defined as the "glacier catchment" for the duration of the simulation. That is, the portion of a basin within a glacier catchment does not change over time, even as the area of the glacier itself does change. Runoff is simulated at the individual glacier level and includes all water exiting the catchment, both melted snow and ice as well as rain falling within the catchment boundary. These monthly glacier runoff totals are then aggregated to the basin scale.

In the Huss and Hock (2018) glacial model output, some portion of the GCM-derived precipitation falling within a basin is also counted within the basin glacial runoff. To avoid double-counting precipitation in our SPEI_G moisture source term, we scale GCM-derived precipitation by each basin's unglaciated area (Equation 1) and add it to glacial runoff scaled by the basin's glaciated area. PET is then subtracted from this sum, which is equivalent to assuming that both precipitation falling in the unglaciated part of the basin and glacial runoff from the glaciated part of the basin are encountering atmospheric demand for moisture.

Text S3. Quantifying ensemble mean and range

In the present study, we have focused on identifying and interpreting qualitative differences among GCM-projected SPEI with and without glacial runoff. This approach makes evident, for example, that no one GCM is consistently wetter or drier than another across basins, and that differences in both land and atmosphere schemes shape projected SPEI in glaciated basins (see main text).

Future studies of hydrological drought in glaciated basins may wish to quantify inter-basin differences in the glacial effect. To that end, we have supplied code in our public repository to compute the inter-GCM mean and interquartile range of SPEI for each basin, emissions scenario, and inclusion/exclusion of glacial runoff—the so-called structural uncertainty in the glacial effect.

Figure S5 plots these ensemble statistics for the Tarim Basin, both with and without glacial runoff (compare with main text Figure 1). The ensemble mean and interquartile range further reinforce the findings of the main text: without glacial runoff, the Tarim basin would be drying throughout the century, while with glacial runoff conditions are projected to be wetter in the 21st century than the 20th.

Figure S2. Glacial effect on 30-year running mean SPEI by basin, for all 56 large-scale glaciated basins worldwide, under emissions scenario RCP 4.5. Figures are styled in the same way as main text Figure 2: Curves shown are a 30-year running mean of the difference SPEI_W- SPEI_N, where "W" and "N" denote "with glacial runoff" and "no accounting for glaciers", respectively. A different vertical scale has been applied to each plot to aid readability. Grey shading indicates the period when 30-year running means include years for which the glacier model has not yet been switched on.

Figure S3. Glacial effect on 30-year running SPEI variance by basin, for all 56 large-scale glaciated basins worldwide, under emissions scenario RCP 4.5. Figures are styled in the same way as main text Figure 3: Curves shown are the difference of running 30-year variances, $\mathrm{Var}(\mathrm{SPEI}_W)$-$\mathrm{Var}(\mathrm{SPEI}_N)$, where "W" and "N" denote "with glacial runoff" and "no accounting for glaciers", respectively. A different vertical scale has been applied to each plot to aid readability. Grey shading indicates the period when 30-year running statistics include years for which the glacier model has not yet been switched on.

References

Allen, R. G., Pereira, L. S., Raes, D., & Smith, M. (1998). Crop evapotranspiration—guidelines for computing crop water requirements. In *FAO Irrigation and drainage paper* (Vol. 56). United Nations Food and Agriculture Organization.

Cook, B. I., Smerdon, J. E., Seager, R., & Coats, S. (2014). Global warming and 21st century drying. *Climate Dynamics*, *43*(9-10), 2607–2627. doi: 10.1007/s00382-014-2075-y

Dee, D. P., Uppala, S. M., Simmons, A. J., Berrisford, P., Poli, P., Kobayashi, S., ... Vitart, F. (2011). The ERA-Interim reanalysis: configuration and performance of the data assimilation system. *Quarterly Journal of the Royal Meteorological Society*, *137*(656), 553–597. doi: 10.1002/qj.828

Huss, M., & Hock, R. (2018). Global-scale hydrological response to future glacier mass loss. *Nature Climate Change*, *8*(2), 135–140. doi: 10.1038/s41558-017-0049-x

McEvoy, D. J., Huntington, J. L., Abatzoglou, J. T., & Edwards, L. M. (2012). An evaluation of multiscalar drought indices in Nevada and Eastern California. *Earth Interactions*, *16*(18), 1–18.

McKee, T. B., Doesken, N. J., & Kleist, J. (1993). The relationship of drought frequency and duration to time scales. In *Proceedings of the 8th Conference on Applied Climatology, 17-22 January 1993, Anaheim, CA.* Boston, MA.

Milly, P. C., & Dunne, K. A. (2016). Potential evapotranspiration and continental drying. *Nature Climate Change*, *6*(10), 946. doi: 10.1038/nclimate3046

Taylor, K. E., Stouffer, R. J., & Meehl, G. A. (2011). An overview of CMIP5 and the experiment design. *Bulletin of the American Meteorological Society*, *93*(4), 485–498. doi: 10.1175/BAMS-D-11-00094.1

Vicente-Serrano, S. M., Beguería, S., & López-Moreno, J. I. (2009). A multiscalar drought index sensitive to global warming: The standardized precipitation evapotranspiration index. *Journal of Climate*, *23*(7), 1696–1718. doi: 10.1175/2009JCLI2909.1

World Meteorological Organization, & Global Water Partnership. (2016). *Handbook of drought indicators and indices* (Tech. Rep.). Geneva, Switzerland: Integrated Drought Management Programme (IDMP).

Yang, Y., Roderick, M. L., Zhang, S., McVicar, T. R., & Donohue, R. J. (2019). Hydrologic implications of vegetation response to elevated CO2 in climate projections. *Nature Climate Change*, *9*(1), 44. doi: 10.1038/s41558-018-0361-0

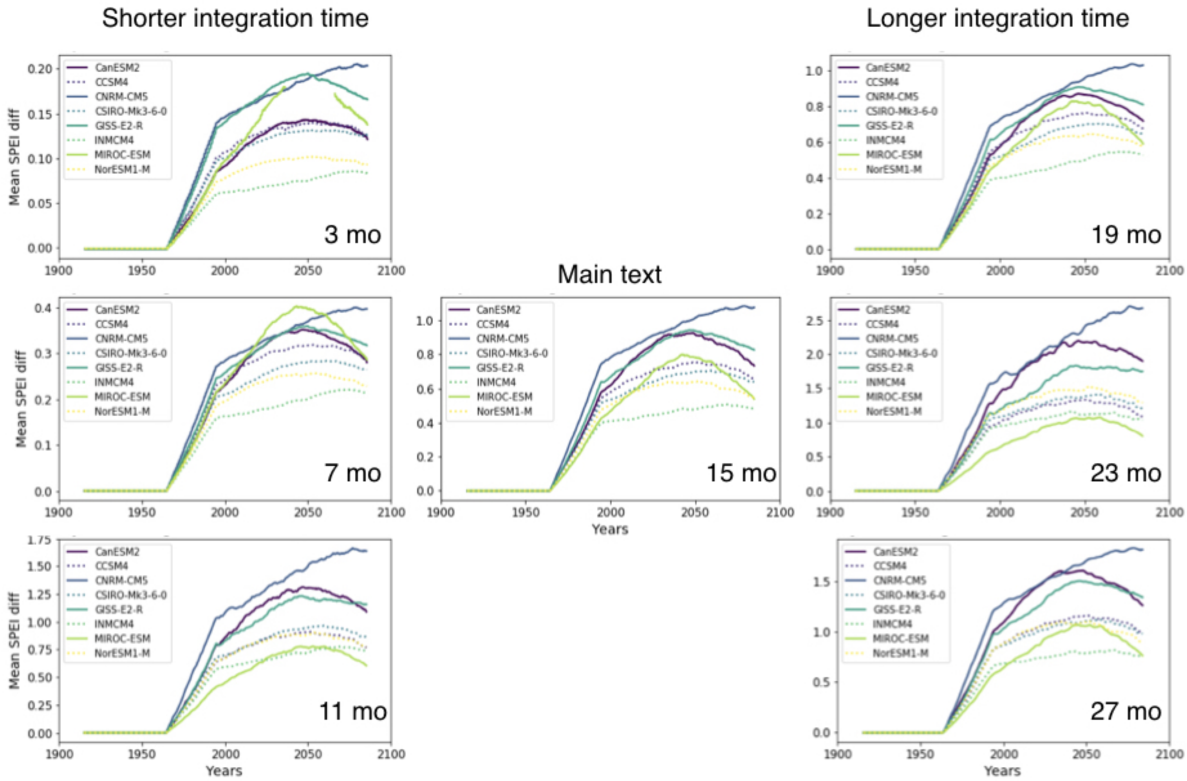

Figure S1. Comparison of glacial effect on SPEI over the 21st century when SPEI is computed with integration timescales ranging from 3 to 27 months. The central panel shows the 15-month integration timescale analysed in the main text of this work; shorter integration timescales appear to the left and longer timescales to the right. Note different y-axis scales in different panels.

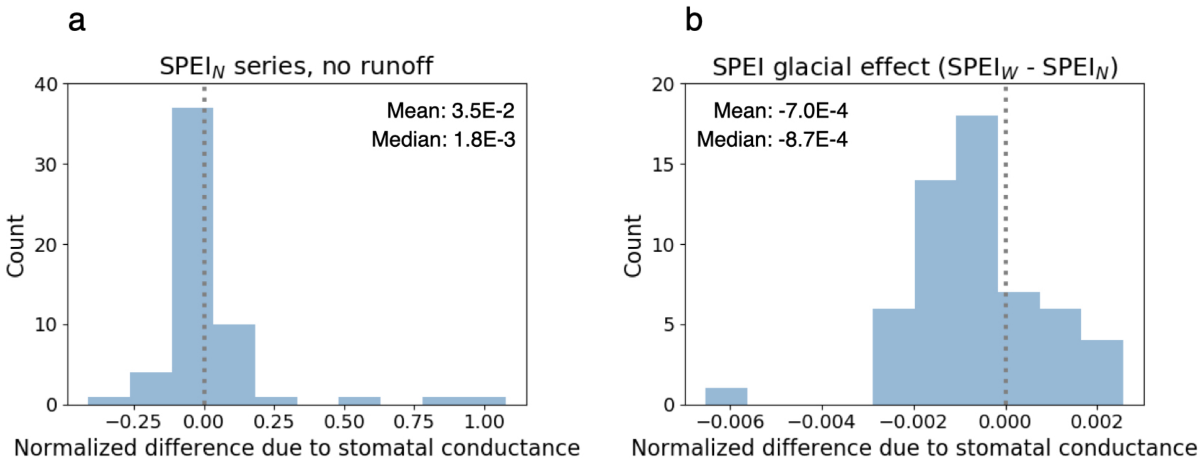

Figure S4. Histograms of pairwise percent difference after accounting for variable stomatal conductance in (a) SPEI_N, the SPEI timeseries for each basin computed with no glacial runoff, and (b) $\mathrm{SPEI}_W - \mathrm{SPEI}_N$, the glacial effect on SPEI timeseries for each basin.

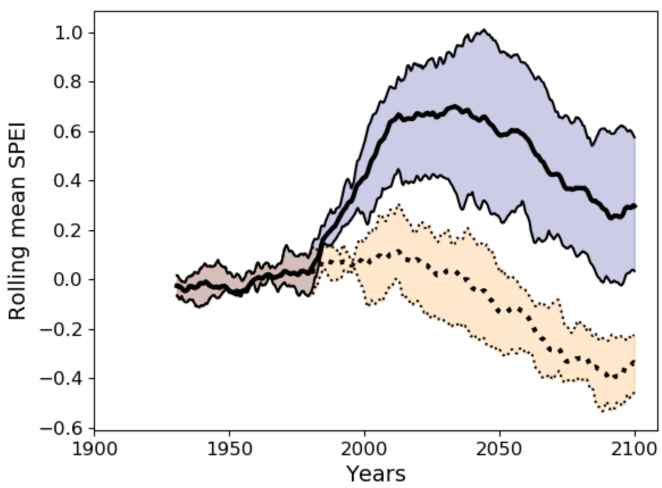

Figure S5. Multi-GCM ensemble mean and interquartile range of SPEI for the Tarim basin, with (solid, blue fill) and without (dashed, orange fill) glacial runoff.